

## Investigation methods for analysis of transient phenomena concerning design and operation of hydraulic-machine systems—A review



Deyou Li<sup>a</sup>, Xiaolong Fu<sup>a</sup>, Zhigang Zuo<sup>b,\*</sup>, Hongjie Wang<sup>a,\*</sup>, Zhenggui Li<sup>c</sup>, Shuhong Liu<sup>b</sup>, Xianzhu Wei<sup>d</sup>

<sup>a</sup> School of Energy Science and Engineering, Harbin Institute of Technology, Harbin 150001, China

<sup>b</sup> State Key Laboratory of Hydrosience and Engineering, Department of Energy and Power Engineering, Tsinghua University, Beijing 100084, China

<sup>c</sup> Key Laboratory of Fluid and Power Machinery (Xihua University), Ministry of Education Sichuan, Chengdu 610039, China

<sup>d</sup> State Key Laboratory of Hydro-Power Equipment, Harbin Institute of Large Electrical Machinery, Harbin 150040, China

### ARTICLE INFO

#### Keywords:

Hydraulic-machine systems  
Transient processes  
Simulation strategies  
Transient characteristics

### ABSTRACT

Over the past decade, the use of conventional one-dimensional numerical-simulation methods has been demonstrated to be inadequate in terms of their usefulness in investigations concerning transient processes in hydraulic machines systems—their theoretical analyses and engineering applications. Consequently, numerous three-dimensional numerical methods capable of accurately simulating transient processes in hydraulic-machine systems have been proposed and improved upon in recent years. Through use of these novel methods and strategies, many researchers have investigated transient characteristics of processes occurring within hydraulic-machine systems along with corresponding formation mechanisms. This study presents a comprehensive review of related experimental studies, novel numerical methods and strategies along with transient characteristics and formation mechanisms in hydraulic-machine systems. Based on this study, suggestions have been made concerning the selection of simulation methods to be used and directions for future research have been proposed.

### 1. Introduction

Hydraulic power generation, among sustainable renewable-energy sources, has been recognized as a proven, extremely flexible, and well-advanced grid-regulating technology [1]. In particular, hydropower-pumped storage has been recognized as, perhaps, the only commercially proven grid-scale energy-storage technique [2–4]. Hydraulic machines, without doubt, play a significant role in hydraulic power generation, and key devices include hydro-turbines [5], pump-turbines [6–10], and pumps [11–13]. The past few years have witnessed an increasing investment in renewable energy sources—wind and solar power. In order to achieve load levelling, grid-frequency regulation, and reserve spinning, hydraulic machines in hydropower stations frequently perform transient processes [14,15].

Transient processes of hydraulic machines involve a series of transitions, wherein hydraulic machines undergo a transformation in their operating mode from one stable state of operation to another. Pump-turbines, in particular, undergo all types of transient processes during their typical four-quadrant operations, as depicted in Fig. 1.

Pump-turbines, during their operation as a pump, may undergo

such processes as pump start-up, shutdown, and pump power failure. In the event of a pump power failure, if the guide vanes malfunction, pump-turbines perform a pump runaway process along a dynamic trajectory, as depicted by the hill chart in Fig. 2.

In contrast, during operation as hydro-turbines, pump-turbines may undergo such processes as hydro-turbine start-up [18], shutdown [19], and load acceptance and rejection processes [20]. At the end of hydro-turbine load rejection, if guide vanes malfunction, the pump-turbine performs a runaway oscillation process, as depicted in Fig. 3 [21].

During transient processes, especially near the speed-no-load condition (when hydraulic torque on runner equals zero), the pump-turbine demonstrates serious fluctuation characteristics, and a series of water-hammer phenomena may occur within water-conveyance pipeline systems. The large rise in pressure head and severe fluctuations caused by water-hammer phenomena directly impact the safe and stable operation of pumped-storage power stations. In fact, even rotating parts of hydraulic machines tend to be lifted by unbalanced axial-reaction forces generated by leakage flows in the sidewall clearance as well as the reverse water hammer within the draft tube. For example, in 2003, rotating parts of hydraulic machines installed in the

\* Corresponding authors.

E-mail addresses: [lidayou@hit.edu.cn](mailto:lidayou@hit.edu.cn) (D. Li), [fuxiaolonghit@163.com](mailto:fuxiaolonghit@163.com) (X. Fu), [zhigang200@tsinghua.edu.cn](mailto:zhigang200@tsinghua.edu.cn) (Z. Zuo), [wanghongjie@hit.edu.cn](mailto:wanghongjie@hit.edu.cn) (H. Wang), [lzhgui@mail.xhu.edu.cn](mailto:lzhgui@mail.xhu.edu.cn) (Z. Li), [liushuhong@mail.tsinghua.edu.cn](mailto:liushuhong@mail.tsinghua.edu.cn) (S. Liu), [wzx@hec-china.com](mailto:wzx@hec-china.com) (X. Wei).

<https://doi.org/10.1016/j.rser.2018.10.023>

Received 19 August 2018; Received in revised form 6 October 2018; Accepted 19 October 2018

1364-0321/ © 2018 Elsevier Ltd. All rights reserved.

**Abbreviation and nomenclature**

$A$	cross section of pipeline, $m^2$	$P$	Reynolds averaged pressure, Pa
$a$	water hammer wave speed, $m s^{-1}$	$P_m, P_{out}$	output power, J
$a_0$	water hammer wave speed at initial state, $m s^{-1}$	$p$	pressure, Pa
$a_{01}, a_{02}, a_{0n}$	several different guide vane opening, degrees	$p_0$	pressure at initial state, Pa
$B$	$B = a/(gA)$	$p_E, p^*(t)$	non-dimensional pressure fluctuation
BEP	best efficiency point	$p(t)$	original transient pressure signal, Pa
$c$	coefficient related to the anchored condition and the wall thickness of the pipe	$\bar{p}(t)$	averaged pressure, Pa
$c_p$	pressure coefficient	$\bar{p}$	pressure, Pa
$c_{pl}$	pressure coefficient at low frequency	PS	blade pressure side
$c_{ph}$	pressure coefficient at high frequency	$Q$	flow rate, $m^3 s^{-1}$
$D$	diameter of pipeline, m	$q_{11}, Q_{11}, Q_{ed}, Q_{ED}$	unite discharge
$E$	specific hydraulic energy of turbine or Young's modulus of elasticity of the pipe-wall	$Q_M^{(n)}$	discharge of node M at the $n_{th}$ time step, $m^3 s^{-1}$
$e$	pipe-wall thickness, mm	$Q_P^{(n+1)}$	discharge of node P at the $(n + 1)_{th}$ time step, $m^3 s^{-1}$
$F$	frequency, Hz	$Q_S^{(n)}$	discharge of node S at the $n_{th}$ time step, $m^3 s^{-1}$
$Force_x$	radial force in x direction, N	$Q_{1-1}^{(n)}$	discharge of section 1–1 at the $n_{th}$ time step, $m^3 s^{-1}$
$Force_y$	radial force in y direction, N	$Q_{1-1}^{(n+1)}$	discharge of section 1–1 at the $(n + 1)_{th}$ time step, $m^3 s^{-1}$
$F_z$	axial force, N	SS	blade suction side
$f$	coefficient of friction resistance	$T, t$	time, s
$f_i$	body force component	$T_{ED}$	unite torque
$g$	gravity acceleration, $m s^{-2}$	$\Theta$	ball valve angular position, degrees
$H$	head, m	$U/U_0$	normalized velocity
$H_d$	pressure head at draft-tube inlet, m	$U_i, U_j$	Reynolds averaged velocity component, $m s^{-1}$
$H_M^{(n)}$	pressure head of node M at the $n_{th}$ time step, m	$u_i, u_j$	transient velocity component, $m s^{-1}$
$H_P^{(n+1)}$	pressure head of node P at the $(n + 1)_{th}$ time step, m	$V, V_P, V_R, V_S$	velocity, $m s^{-1}$
$H_S^{(n)}$	pressure head of node S at the $n_{th}$ time step, m	$x$	x coordinate
$H_{1-1}^{(n)}$	pressure head of section 1–1 at the $n_{th}$ time step, m	$x_b, x_j$	Cartesian coordinate component
$H_{1-1}^{(n+1)}$	pressure head of section 1–1 at the $(n + 1)_{th}$ time step, m	$y$	y coordinate
$H_{2-2}^{(n)}$	pressure head of section 2–2 at the $n_{th}$ time step, m	$\alpha, \alpha_{GV}$	guide vane angular position, degrees
$H_s$	pressure head at spiral-casing inlet, m	$\alpha_1, \alpha_2$	respectively the volume fraction of water and air, %
$H(t)$	transient head of hydraulic machinery, m	$\beta$	angle between the axis of pipeline and horizontal plane, degrees
$I, J$	inertia of the rotor, $kg m^2$	$\omega$	angular speed, $rad s^{-1}$
$i$	node number or time step number	$\omega_g$	angular speed of guide vane, $rad s^{-1}$
$K$	bulk modulus of elasticity	$\rho$	density, $kg m^{-3}$
$K_{cm1}$	flow rate coefficient	$\rho_0$	density at initial state, $kg m^{-3}$
$K_{u1}$	velocity coefficient	$\rho_1, \rho_2$	respectively the density of water and air, $kg m^{-3}$
$M, M_z$	resultant torque on rotor in axial direction, N m	$(\rho E)_{BEP}$	specific hydraulic energy level at best efficiency point, $J kg^{-1}$
$M_f$	resultant torque of friction and wind resistance torque, N m	$-\rho \overline{u'_i u'_j}$	Reynolds stress component, Pa
$M_g$	electromagnetic torque on rotor, N m	$\eta$	turbine efficiency, %
$M_t$	hydraulic torque on rotor, N m	$\mu_1, \mu_2$	respectively the dynamic viscosity of water and air, $N s m^{-2}$
$M_{11}$	unit torque, N m	$\nu$	kinematic viscosity of water, $m^2 s^{-1}$
$n$	rotational speed, $r min^{-1}$	$\Phi, \Phi_0$	each parameter presented in the plot and its initial value
$n_{11}, n_{ed}, n_{ED}$	unite speed, $r min^{-1}$	$\Delta$	increment
		$\Delta P$	pressure increment, %

Tianhuangping pumped-storage power station in China were lifted during the load acceptance process, thereby resulting in severe wear and tear of the labyrinth sealing device on the hub side [22].

To ensure safe and stable operation of hydropower stations, significant researches involving experiments and numerical simulations have been performed with major focus on investigating transient processes that occur in hydraulic machines.

## 2. Experimental investigation of transient process

Experimental investigations of transient processes that occur in hydraulic machines are rare when compared against investigations based on numerical simulations. That said, experimental studies are very important for understanding the mechanisms underlying transient processes.

### 2.1. Experimental rules and measurement parameters

All on-field and model experiments concerning transient processes cited in this review have been performed in accordance with the standards of International Electrotechnical Commission (IEC) [23,24]. Some primary measurement parameters of concern when performing tests for transient processes include rotational speed, resultant torque on rotor, water head, discharge, and pressure, as depicted in Fig. 4. Among these measurement parameters, pressure fluctuations reflect transient characteristics of hydraulic machines more clearly. Consequently, pressure fluctuations usually form the primary research focus during experiments involving transient hydraulic-machine processes.

## 2.2. Experimental investigation of pressure fluctuations

### 2.2.1. Monitor points or pressure signals

During pressure fluctuation tests, certain locations within the vaneless space, runner, and draft-tube are usually selected to monitor pressure signals during the transient process under study, as depicted in Fig. 5.

### 2.2.2. Method of processing transient pressure signals

After obtaining raw data containing experimental pressure signals, a team of investigators directly analyses time and frequency characteristics of the original experimental data to deduce transient fluctuating characteristics of the hydraulic machine. Simultaneously, another team of investigators analyses time and frequency characteristics of non-dimensional pressure fluctuations. These non-dimensional pressure fluctuations could be obtained through use of two calculation formulae expressed below as Eqs. (1) [26] and (2) [25,27].

$$p_E = \frac{p(t) - \bar{p}(t)}{(\rho E)_{BEP}} \quad (1)$$

where  $p_E$  denotes the non-dimensional pressure fluctuation;  $p(t)$  refers to the original transient pressure signal (Pa);  $\bar{p}(t)$  denotes average pressure (Pa); and  $(\rho E)_{BEP}$  denotes the specific hydraulic energy level ( $J\ kg^{-1}$ ) at the best efficiency point (BEP).

$$p^*(t) = \frac{p(t) - \bar{p}(t)}{\rho g H(t)} \quad (2)$$

Here,  $p^*(t)$  denotes the non-dimensional pressure fluctuation;  $\rho$  denotes the density of water ( $kg\ m^{-3}$ );  $g$  denotes acceleration due to gravity ( $m\ s^{-2}$ ); and  $H(t)$  denotes transient head of the hydraulic machine (m).

### 2.2.3. Results of pressure fluctuation investigations

Through adoption of the above-mentioned technique, few pressure-fluctuation experiments have been performed in extant studies to investigate the transient pulsating characteristics of hydraulic machines. Trivedi et al. [28–31] measured the pressure fluctuations that occur within Francis turbines during transient operations, and their findings indicated that the maximum amplitude of pressure fluctuations and pressure load on runner blades during transient operations was much greater compared to that during operation at the best efficiency point. For instance, the pressure load and maximum amplitude of pressure fluctuations on runner blades under runaway conditions were, respectively, observed to be 3 and 2.6 times higher compared to their corresponding values at the best efficiency point, as depicted in Fig. 6. Especially, during guide-vane movement, corresponding pressure fluctuations were usually observed to be more serious, as depicted in Fig. 7.

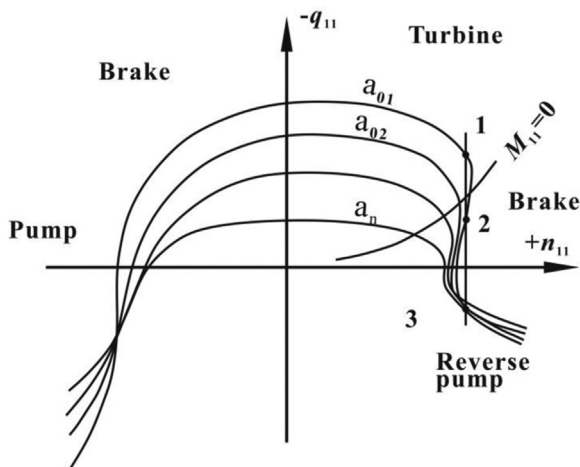


Fig. 1. Four-quadrant characteristics of pump-turbines [16].

High-pressure fluctuations and increased loads on runner blades result in generation of cyclic stresses and fatigue development within the runner. These effects tend to shorten the service life of Francis turbines. Although such transient processes cannot be avoided, the operating life of Francis turbines could be improved by minimizing the undesirable pressure fluctuations and loadings on runner blades during transient operations. This could be realized through use of certain effective control strategies, such as improved shutdown and guide-vane movement in accordance with a control law [32,33], as depicted in Fig. 8.

Amiri et al. [35] investigated the effect of unsteady pressures on the runner of a Kaplan turbine during load acceptance and rejection phases. In their study, during load acceptance, the variation process was observed to be relatively smooth. During load rejection, however, the situation was observed to be completely different. Between high loads and BEP, the transient process continuously demonstrated a relatively low increase in amplitude, as depicted in Fig. 9(a). From high loads to part loads, the increase in amplitude was observed to be relatively high, and the transient process was quite unstable, as depicted in Fig. 9(b). Houde et al. [36] experimentally investigated the effects of transient pressure fluctuations on propeller runner blades. Their results indicate that the transition from normal operating conditions to speed-no-load conditions is also unstable.

Further, Yang et al. [37] analysed, in detail, frequency components and excitation sources of transient pressure fluctuations in a prototype Francis pump-turbine. Their analysis indicated that high-frequency pressure fluctuations are caused by effects of rotor-stator interactions. Additionally, they observed that low-frequency pressure fluctuations are closely related to the rotating stall phenomenon within vaneless space and complex flow patterns within the draft tube shown in Fig. 10. Ruchonnet and Braun [38] performed tests on transient transition processes (from pump operation to turbine and vice versa) on a reduced-scale pump-turbine. Their experimental results demonstrated frequency characteristics similar to those observed in prototype tests.

In pumped-storage power plants wherein multiple machines share the same main pipes, once a given pump-turbine rejects its load, other pump-turbines also follow suit. This process is defined as one after another (OAA) load rejection. Under OAA conditions, hydraulic connections between units experience higher water-hammer pressure, thereby directly threatens the safety of pumped-storage power plants. Zeng et al. [39] investigated the effects of S-shaped pump-turbine characteristics on transient pressure under OAA conditions, as depicted in Fig. 11.

## 2.3. Internal flow experiments

With regard to experiments performed concerning internal flow patterns during transient processes, Li [40] performed experimental

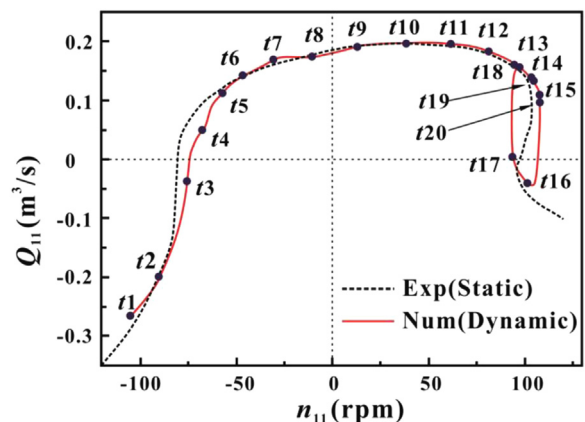


Fig. 2. Hill chart of pump-turbine during pump runaway caused by power failure [17].

investigations during start-up process of a centrifugal pump. Test results obtained via particle image velocimetry (PIV) demonstrate that internal unsteady flow patterns are basically consistent with performance characteristics of the pump, as shown in Fig. 12. This indicates that internal unsteady flow patterns directly influence transient performance characteristics.

### 3. Numerical simulation investigation of transient process

On one hand, it is almost impossible for researchers to investigate transient processes in hydraulic machines using experimental methods. On the other hand, it is more convenient to extract flow information at any location through use of numerical methods rather than actual experiments. Consequently, method of numerical simulation has also been adopted in extant researches to investigate transient processes. To understand up-to-date research status and identify gaps in the research of transient processes via simulation, this study reviews relevant numerical studies involving transient processes conducted over the last decade.

To date, three primary methods have been proposed and developed to simulate transient process. These methods differ from each other in terms of their dimensions of spatial computational domains and can each be summarized as follows.

#### 3.1. One-dimensional (1-D) simulation of transient flow

##### 3.1.1. Governing equation for 1-D transient flow and numerical solution

Previously, to save on computational resources, 1-D methods were adopted to simulate transient processes that occur within hydropower stations or pump stations comprising long water-conveyance pipelines [41,42]. These 1-D simulation methods were generally based on three assumptions—(1) all spatial computational domains are simplified as 1-D pipelines; (2) water flows within pressurized pipelines and pipeline walls are elastic; (3) effects of cavitation are neglected [43,44]. Based on these assumptions, transient flows could be described using following governing equations.

$$\frac{\partial V}{\partial t} + V \frac{\partial V}{\partial x} + g \frac{\partial H}{\partial x} + \frac{f}{2D} V|V| = 0 \quad (3)$$

$$V \frac{\partial H}{\partial x} + \frac{\partial H}{\partial t} + \frac{a^2}{g} \frac{\partial V}{\partial x} + V \sin \beta = 0 \quad (4)$$

Here,  $H$  denotes the pressure head (m);  $V$  denotes velocity (m/s);  $t$  denotes time (s);  $x$  represents the distance along the pipeline axis (m);  $g$  denotes acceleration due to gravity ( $m/s^2$ );  $f$  is the coefficient of friction;  $D$  refers to pipeline diameter (m);  $\beta$  denotes water-hammer wave speed (m/s);  $a$  represents the angle between pipeline axis and horizontal plane (degrees). Adopting the method of characteristics (MOC)

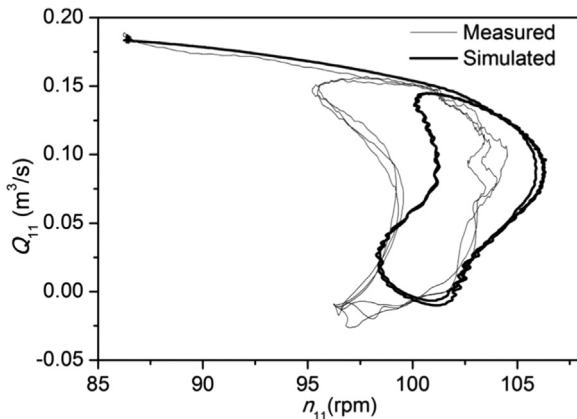


Fig. 3. Runaway-oscillation process [21].

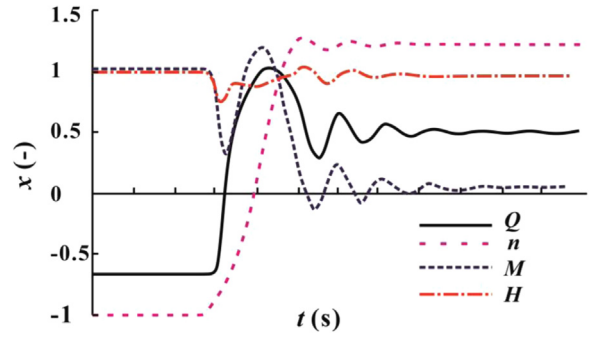


Fig. 4. Primary measurement parameters involved in transient hydraulic-machine processes [25].

[45], as shown in Fig. 13, the difference solution  $V_p$  and  $H_p$  for Eqs. (3) and (4) could be obtained for most flow domains except across certain specific boundaries, such as inlet, outlet, surge tank, and hydro-turbines etc. Values of  $V_p$  and  $H_p$  could be obtained using following equations.

$$V_p = 0.5 \left[ V_R + V_S + \frac{g}{a} (H_R - H_S) - \frac{g}{a} \Delta t \sin \beta (V_R - V_S) - \frac{f \Delta t}{2D} (V_R |V_R| + V_S |V_S|) \right] \quad (5)$$

$$H_p = 0.5 \left[ H_R + H_S + \frac{a}{g} (V_R - V_S) - \Delta t \sin \beta (V_R + V_S) - \frac{a f \Delta t}{g 2D} (V_R |V_R| - V_S |V_S|) \right] \quad (6)$$

##### 3.1.2. Solution of hydraulic machine boundary condition

When using MOC, the hydro-turbine boundary condition causes one of the most crucial issues [46]. In 1-D MOC, two methods are primarily used to solve for transient processes that occur at hydro-turbine boundaries. The first is called the interpolation method based on the static complete characteristic curve [44]. Owing to the cross, gather, and reverse operation of guide-vane opening lines of pump-turbines operating in the pump mode and reverse-pump modes [47], interpolation errors incurred are relatively large and cannot not be neglected. Some countermeasures, such as Suter transformation [48] and complete characteristic space surface fitting [47,49], have been adopted to reduce interpolation errors. Nonetheless, interpolation errors cannot be completely eliminated. Another method to address hydro-turbine boundary conditions is the 1-D analytical method of internal characteristics [50]. In this method, the derivation of generalized 1-D Euler equation [50,51] introduces two assumptions—(1) the flow within hydro-turbines 1-D and inviscid; (2) flow is axisymmetric. However, these assumptions are inconsistent with reality, and therefore, this treatment of hydro-turbine boundary condition is also inaccurate.

In addition, 1-D MOC is an explicit numerical method, and its ideal solution relies on adequately small time-step sizes. Most importantly, 1-D MOC is a simplified 1-D method. As such, many complex nonlinear pulsation characteristics of transient processes cannot be captured and reproduced through use of this method.

#### 3.2. Three-dimensional (3-D) flow simulation in water-conveyance system

##### 3.2.1. Governing equations for 3-D single-phase flow and numerical solution

Considering that 1-D numerical techniques cannot accurately simulate nonlinear transient characteristics of transient hydraulic-machine processes, a full 3-D method was proposed to simulate interactions between transient flows in water-conveyance pipelines and

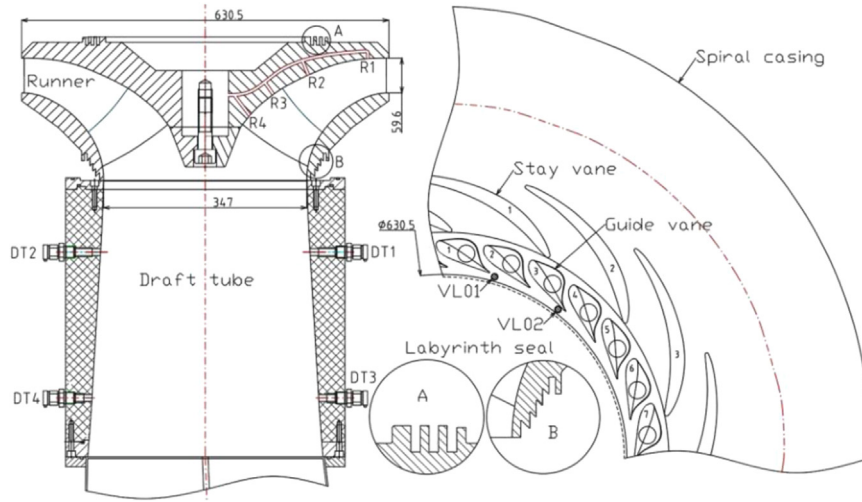


Fig. 5. Monitoring points for pressure fluctuations within a Francis turbine [26].

unsteady turbulent flows within hydraulic machines [52–54]. In particular, in tubular hydraulic machines (refer Fig. 14), the flow passages are relatively short [55]. Three-dimensional flow characteristics are very significant and cannot accurately be simulated using 1-D numerical methods [56]. Therefore, full 3-D methods are necessary to simulate transient flows in tubular hydraulic machines [51,57–59]. In inchoate full 3-D numerical methods, transient flows within 3-D water-conveyance systems are considered incompressible [60]. These incompressible transient flows could be described using the continuity Eq. (7) and momentum Eq. (8) as follows.

$$\frac{\partial u_i}{\partial x_i} = 0 \quad (7)$$

$$\frac{\partial u_i}{\partial t} + u_j \frac{\partial u_i}{\partial x_j} = f_i - \frac{1}{\rho} \frac{\partial p}{\partial x_i} + \nu \nabla^2 u_i \quad (8)$$

Here,  $u_i$  and  $u_j$  are both transient velocity components ( $i, j = 1, 2, 3$ );  $x_i$  and  $x_j$  denote Cartesian coordinate components;  $t$  denotes time;  $f_i$  is the body force component;  $\rho$  denotes the density of water;  $p$  represents the transient pressure; and  $\nu$  is the kinematic viscosity of water.

In computational fluid dynamics (CFD), direct numerical simulation (DNS) of transient turbulent flow within a hydraulic machine would lead to a very high computational cost. To reduce the computational time and number of calculations required to perform transient turbulent-flow simulations, Reynolds adopted the time-averaged method to obtain an averaged turbulent flow [61]. The Reynolds-averaged continuity Eq. (9) and Navier–Stokes (RANS) Eq. (10) could be deduced to the following forms using the transient turbulent flow Eqs. (7) and (8).

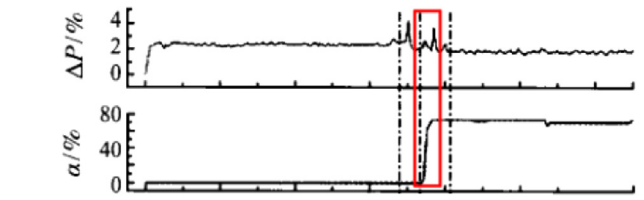


Fig. 7. Pressure fluctuations during pump–turbine start-up in the pump mode [34].

$$\frac{\partial U_i}{\partial x_i} = 0 \quad (9)$$

$$\frac{\partial U_i}{\partial t} + U_j \frac{\partial U_i}{\partial x_j} = f_i - \frac{1}{\rho} \frac{\partial P}{\partial x_i} + \nu \frac{\partial^2 U_i}{\partial x_j^2} + \frac{1}{\rho} \frac{\partial (-\rho \overline{u'_i u'_j})}{\partial x_j} \quad (10)$$

Here,  $U_i$  and  $U_j$  denote Reynolds-averaged velocity components ( $i, j = 1, 2, 3$ );  $P$  refers to Reynolds-averaged pressure; and  $-\rho \overline{u'_i u'_j}$  is the Reynolds stress component. When employing the RANS method, the Reynolds stress terms could be solved for using different turbulence models.

In full 3-D transient-flow simulations of water-conveyance pipeline systems (see Fig. 15), owing to limitation of available computer resources, the adopted computational grid number may not be acceptable when using certain turbulence models. Thus, only the simple one-equation models, such as the Spalart–Allmaras model [62], and two-equation models, such as the  $k-\epsilon$  and share stress transport (SST) models [51,52,56,57], have ever been adopted to simulate transient turbulent flows using the full 3-D method.

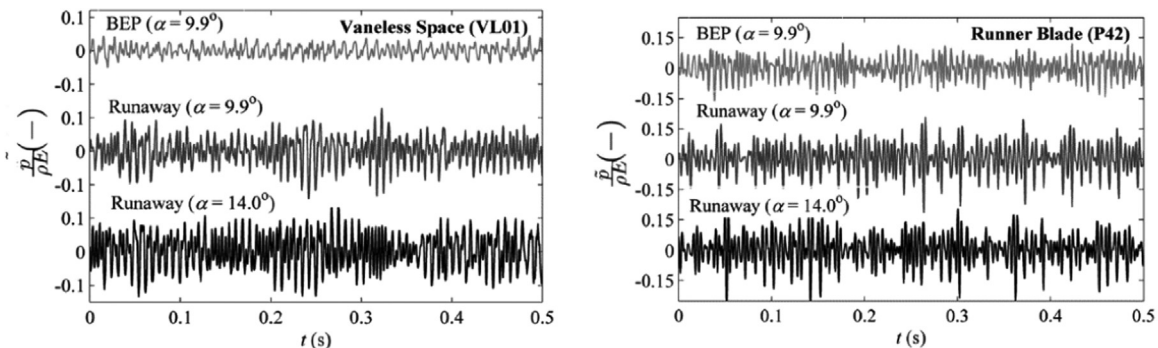
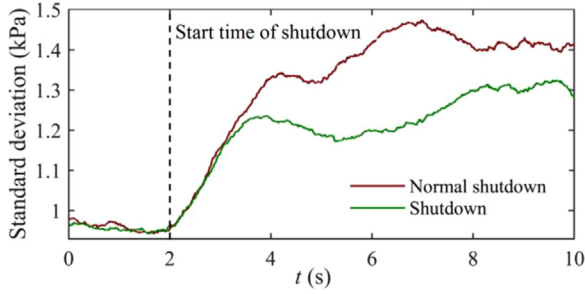
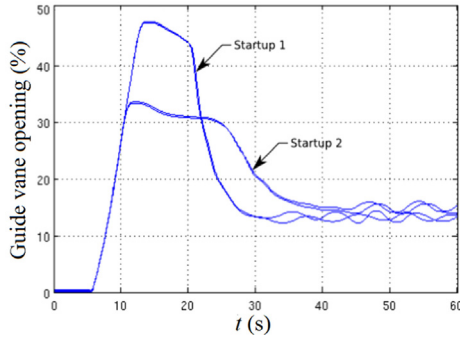


Fig. 6. Comparison of pressure fluctuations under three operating conditions—BEP ( $\alpha = 9.9^\circ$ ); runaway speed at guide-vane angular positions of  $9.9^\circ$  and  $14^\circ$  [29].



(a) Standard deviation in pressure fluctuations within vaneless space under different shutdown modes [32]



(b) Two different start-up schemes for guide-vane opening [33]

Fig. 8. Effective control strategies for minimizing pressure fluctuations and loading of Francis turbine runner blades.

### 3.2.2. Governing equation of 3-D two-phase flow and numerical solution

In most long-distance water-conveyance pipeline systems, surge tanks (refer Fig. 15) are used to reduce the transient water-hammer pressure rise. In such water-conveyance pipeline systems, the buffer effect of surge tanks on transient-pressure increase is usually simulated through use of the volume of fluid (VOF) model [64]. The fluctuating free surface between water and air is tracked by solving continuity Eqs. (11) and (12) to obtain the volume fraction corresponding to each phase [53].

$$\frac{\partial \alpha_1}{\partial t} + \vec{u} \cdot \nabla \alpha_1 = 0 \quad (11)$$

$$\frac{\partial \alpha_2}{\partial t} + \vec{u} \cdot \nabla \alpha_2 = 0 \quad (12)$$

$$\alpha_1 + \alpha_2 = 1 \quad (13)$$

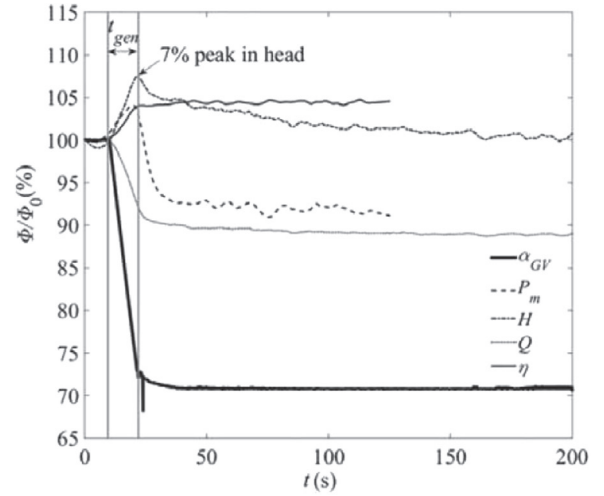
In above equations,  $\alpha_1$  and  $\alpha_2$ , respectively, represent volume fractions of water and air. Velocities obtained by solving single-phase governing Eqs. (9) and (10) are together shared by each phase, and the density and dynamic viscosity property parameters are determined by the volume fraction of each phase in the governing volume as described by following equations.

$$\rho = \rho_1 \alpha_1 + \rho_2 \alpha_2 \quad (14)$$

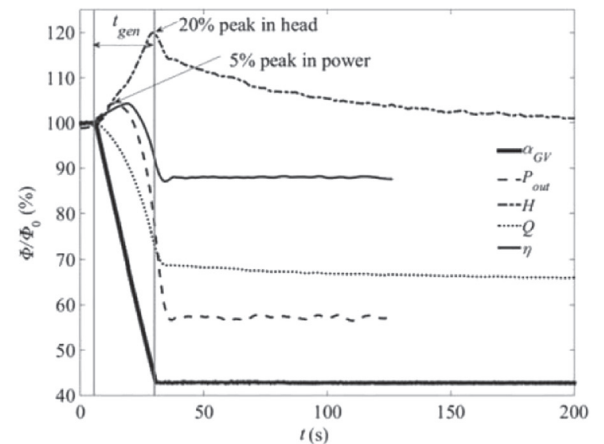
$$\mu = \mu_1 \alpha_1 + \mu_2 \alpha_2 \quad (15)$$

Here,  $\rho_1$  and  $\rho_2$  respectively, denote water and air densities while  $\mu_1$  and  $\mu_2$ , respectively, denote corresponding dynamic viscosities.

A full 3-D two-phase flow simulation uses up a significant amount of computational resources. Consequently, a coupled full 3-D method was proposed to simulate transient two-phase flows within the surge tank and single-phase flow within a resting computational domain, as depicted in Fig. 16 [63]. In the coupled method, the fluctuating free surface between water and air within the surge tank was tracked through adoption of the two-phase VOF model. The transient flow in the resting computational domain can be simulated through adoption of



(a) From high load to best efficiency point



(b) From high load to part load

Fig. 9. Variations in fundamental parameters of Kaplan turbine during load rejection;  $\Phi$  and  $\Phi_0$  refer to parameters presented in the plot and its initial value, respectively [35].

the conventional single-phase flow calculation method. Although the coupled single-phase-VOF (SP-VOF) method serves to save computer resources when compared to the conventional full 3-D two-phase flow-simulation method, it is a full 3-D simulation nonetheless, and as such, it inevitably utilizes substantial computational resources to simulate transient flow in pipeline systems through use of the 3-D method. Under the limitation of available computer resources, use of an inadequately refined computational grid for hydraulic machines would result in that the complex unsteady turbulent flow in hydraulic machines could not be accurately simulated and reproduced. Additionally, in published full 3-D simulations, transient flows in water-conveyance pipeline systems have not been considered incompressible. Consequently, corresponding simulation results could not accurately reflect the actual nonlinear effects of an elastic water hammer.

Cavitation casts a significant effect on transient processes that occur in hydraulic machines [65–68]. However, simulation of cavitation flows in transient processes, once again, requires substantial computational resources. As a result, published researches concerning cavitation in transient turbomachine processes are still rare. As is well recognized, cavitation occurs only on the low-pressure side of hydraulic machines. Analogous to the SP-VOF coupled simulation method, use of a coupled single-phase cavitation simulation method seems to be an attractive alternative to save computer resources.

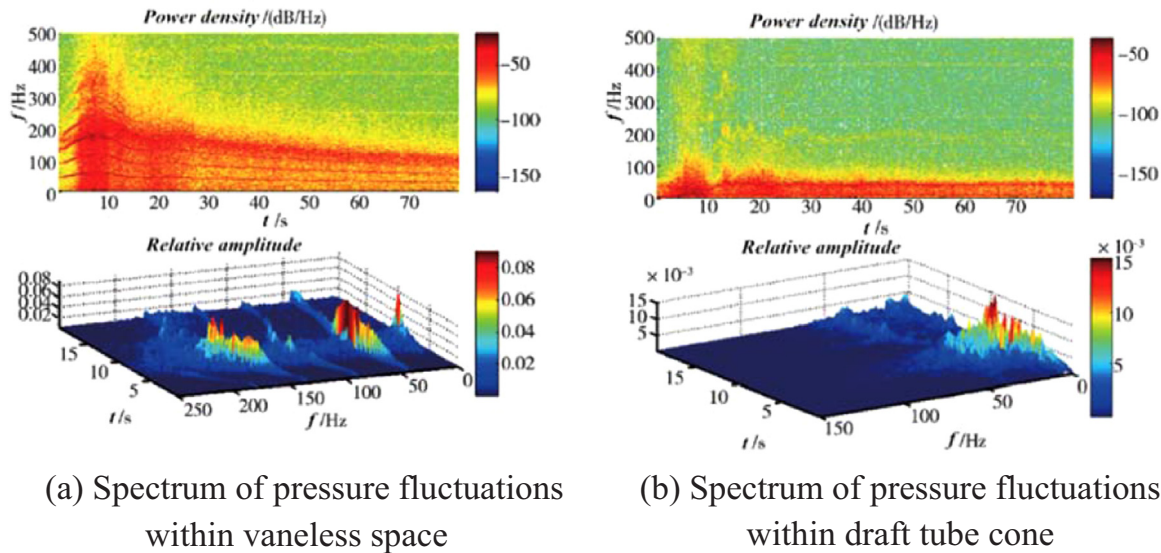


Fig. 10. Short-time Fourier transform results concerning pressure fluctuations during load rejection [37].

### 3.3. 3-D transient-flow simulation in hydraulic machines

To reduce computational costs, some researchers have focused their interest exclusively on hydraulic machines such that they only simulate transient flows within hydraulic machines using the 3-D method. As is well recognized, in most transient processes concerning hydraulic machines, such as start-up, shutdown, and load variation process, guide vanes or valves tend to move and the rotational speed of the runner or impeller fluctuates. These events serve to induce occurrence of the water hammer, which causes severe variations in the transient flow field. Therefore, to accurately simulate unsteady turbulent flows in hydraulic machines via use of the 3-D method, four issues—guide-vane movement, variation in rotational speed with time, unsteady boundary conditions at inlet and outlet of hydraulic machines, and turbulent-flow simulations—must be resolved.

#### 3.3.1. Solution for movement of guide vanes and valves

3.3.1.1. *Dynamic mesh method.* To simulate the movement of guide vanes or valves during transient processes, researchers have presented four different solutions. The first solution for simulating guide-vane

movement is the dynamic mesh method. The dynamic mesh technology is relatively mature, and is widely used to solve moving boundary problems in numerous commercial flow-simulation software (ANSYS Fluent and CFX etc.) [69]. That said, the dynamic mesh method is not the best choice for solving problems involving large deformations and small clearances, because a large grid skewness may cause inaccurate simulation precision when using the dynamic mesh method. For small clearance, refined grids could not be always maintained near the boundary layer each time the mesh is updated.

3.3.1.2. *External grid reconstruction method.* To overcome disadvantages of the dynamic mesh technique, the external grid reconstruction method was proposed in ANSYS CFX [70,71]. Using this method, generation of high-quality refined grids could always be assured to solve problems pertaining to transient hydraulic-machine simulations involving large deformations and small clearances. The mesh quality and external grid reconstruction procedures are depicted in Fig. 17. This method has been successfully applied to simulate transient processes within Francis turbines, pump-turbines, and tubular turbines [57,71,72]. Its only shortcoming is that the external grid

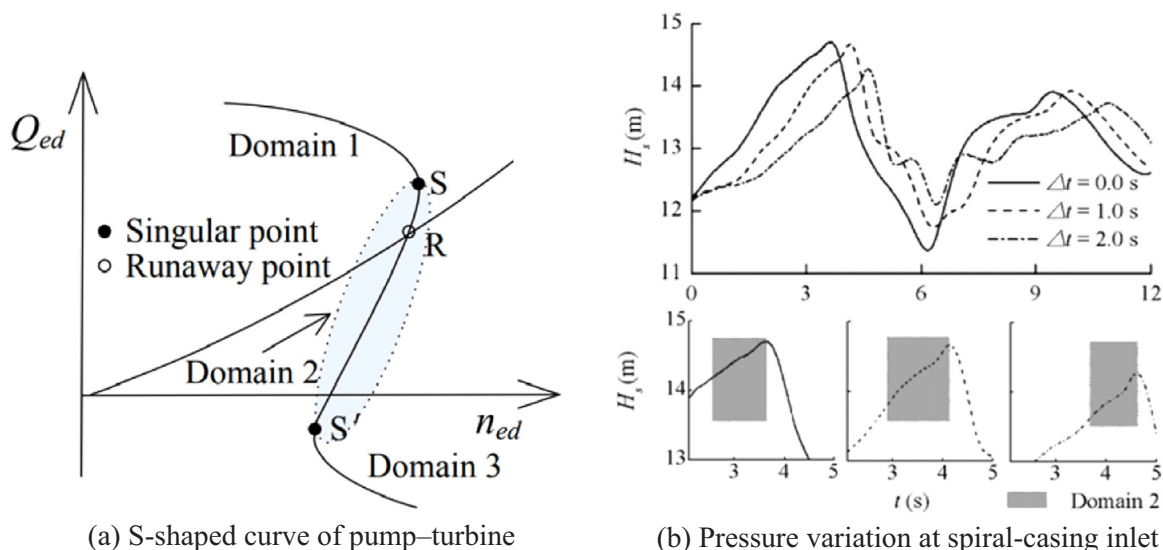


Fig. 11. Effects of S-shaped characteristics of pump-turbine on transient pressure under OAA conditions [39].

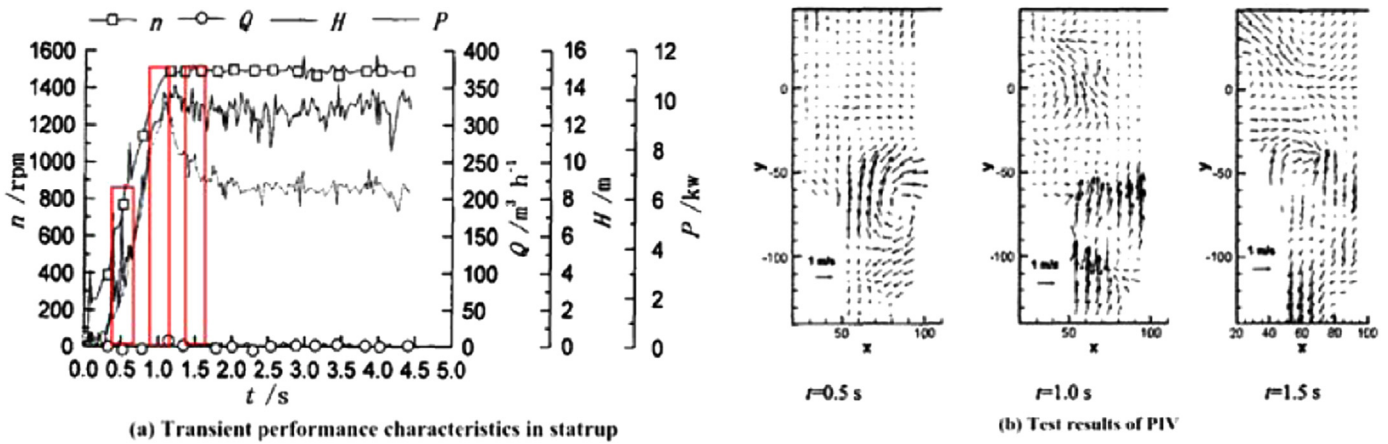


Fig. 12. Experimental test results of centrifugal pump during start-up [40].

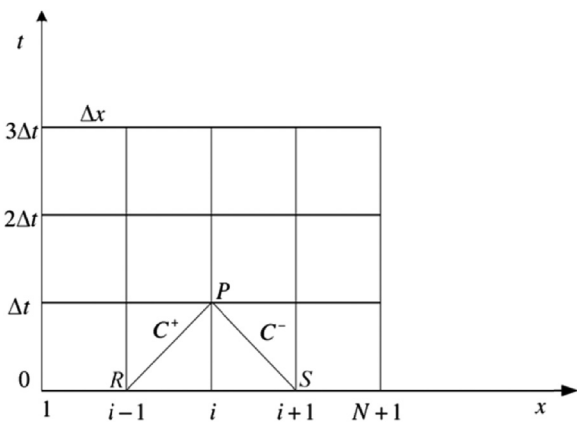


Fig. 13. Difference grid diagram for MOC [44].

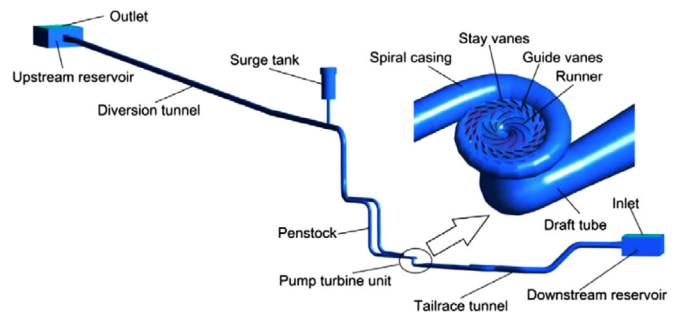


Fig. 15. Pumped-storage power station with long water-conveyance pipeline system and surge tank [63].

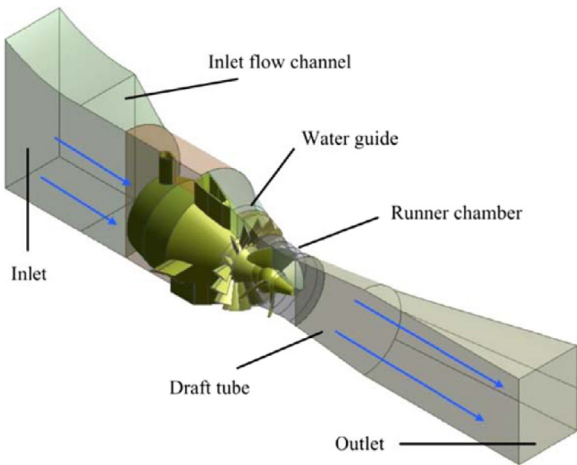


Fig. 14. Flow-passage model of tubular hydraulic turbine [51].

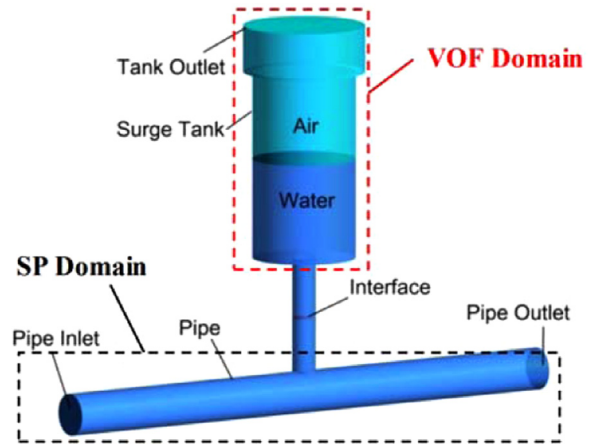


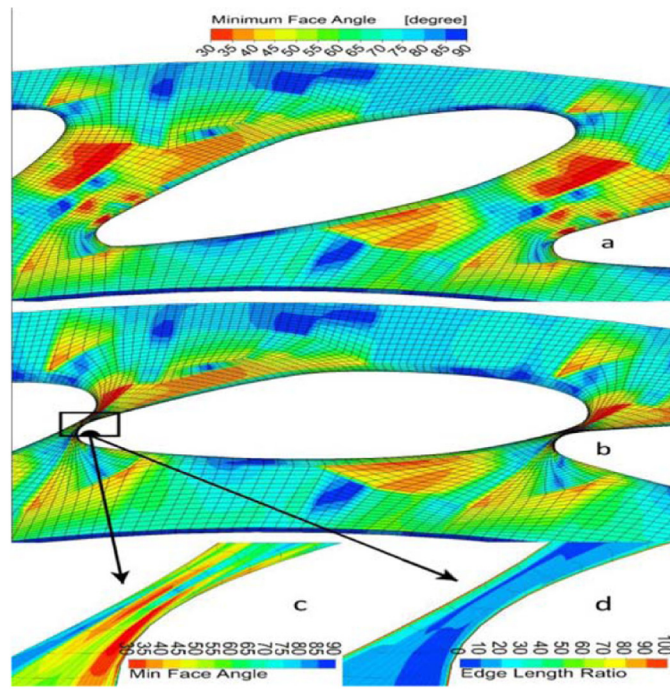
Fig. 16. Coupled computational domain for single-phase water-conveyance pipeline system and two-phase surge tank [63].

reconstruction procedure is relatively complex and takes up considerable simulation time.

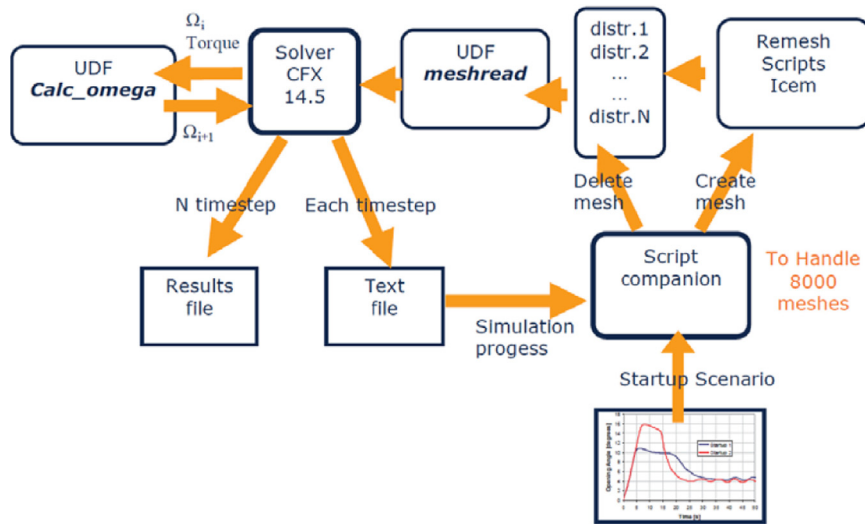
**3.3.1.3. Overset mesh method.** Recently, the overset mesh method has been proposed within the Star CCM+ software package, and the same has been adopted to simulate guide-vane movement in hydraulic machines [18]. Overset meshes comprise static background and moving component meshes, as depicted in Fig. 18. Overset meshes are obtained by excluding the majority of overlapped meshes in the background mesh. These overlapped mesh cells are grouped into active

cells within the computational domain, inactive cells outside the computational domain, and acceptor cells between the background and overlapping meshes. Discretized governing equations, such as Eqs. (9) and (10), are simultaneously solved within active cells, but no equations are solved within inactive cells. The acceptor cells are used to achieve coupling solutions between the background and overset meshes. The overset mesh method always maintains initial high-quality meshes during transient simulations, and has been successfully employed to simulate a number of transient flows with moving or oscillating boundaries [19].

**3.3.1.4. Immersed boundary method.** The immersed boundary method provides solutions to moving boundary problems similar to those



(a) Mesh qualities in terms of minimum face angle and edge length ratio [72].



(b) External grid reconstruction procedure for transient simulations [73].

Fig. 17. Mesh quality and external grid reconstruction procedure.

obtained using the overset mesh method [74]. In this method, the computational grid comprises two sets of meshes—one each in the fluid and solid domains. Different from the overset mesh method, the immersed boundary method solves discretized governing Eqs. (9) and (10) within the entire background fluid mesh. Some specific force source terms are added to the momentum equation to achieve a coupling solution between the fluid and solid domains [75]. In order to accurately simulate boundary-layer flows near solid walls, refined grids must be adopted within the overlapping fluid and solid domains [76]. As is obvious, however, refined grids within the overlapping fluid domain would require additional computer resources. Besides, at present, the immersed boundary method is not adequately mature for use in engineering applications of transient process [77].

### 3.3.2. Solution for variations in rotational speed

Fluctuating rotational speed during transient processes could be described by means of a balanced Eq. (16) in terms of the rotor torque as follows [61].

$$M = M_t + M_g + M_f = J \cdot \frac{d\omega}{dt} \tag{16}$$

$$M_g = \frac{P_{out}}{\omega} \tag{17}$$

Here,  $M$  denotes the resultant torque on rotor;  $M_t$  is the rotor hydraulic torque;  $M_g$  denotes the rotor electromagnetic torque calculated using Eq. (17);  $M_f$  is the resultant friction and wind-resistance torque;  $J$

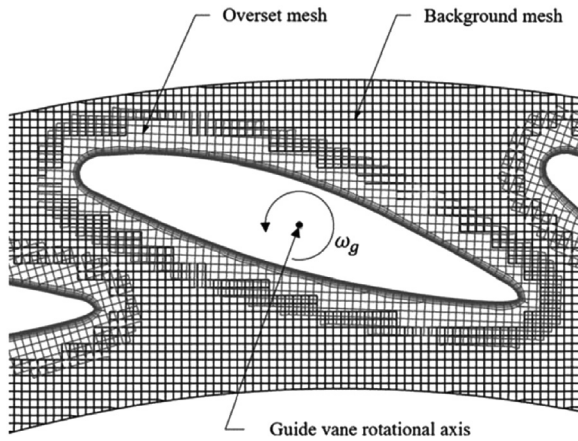


Fig. 18. Background mesh and overset meshes within guide-vane domain [19].

denotes rotor inertia;  $\omega$  is the angular speed of rotor;  $t$  is time; and  $P_{out}$  refers to the output power. Using Eq. (16), an explicit difference solution for the angular speed  $\omega_{i+1}$  could be obtained as follows [78].

$$\omega_{i+1} = \omega_i + \frac{M_{i+1} - M_i}{J} \quad (18)$$

where the subscript  $i$  denotes the time step. The above difference solution represents an explicit scheme. The time-step size should, therefore, be adequately small to assure simulation precision for the rotational speed.

When simulating fluctuating rotational speeds, the multiple rotating reference frame (MRF) and sliding mesh technology represent two frequently-used simulation methods for the rotating domain [62]. Traditionally, use the MRF method has been observed to provide higher computational efficiency. However, it suffers from lower capacity to simulate rotor–stator interactions compared to the sliding mesh technique. Additionally, during flow simulations of rotating machines, the interface (refer Fig. 19) between rotating and static domain forms an important issue, and extant studies suggest that compared to the frozen rotor and stage interface models, use of the transient rotor–stator interface is more suitable for simulating rotor–stator interactions [79]. Given that the type interface also influences transient simulation results, previously mentioned solutions to moving boundary problems could provide a useful means to completely eliminate the interface between rotating and static domains.

The above-mentioned movement of guide vanes and rotor rotation are both problems concerning fluid–body coupling [80]. Fluid–rigid-body coupling is a special type of a simple fluid–structure interaction problem concerning transient processes in hydraulic machines. In fact,

effects of interactions between fluid and elastic structures are pretty significant [81,82]. During transient process in hydraulic machines, amplitudes of fluctuating hydraulic pressures could be as high as several MPa. It is, therefore, necessary to consider interactions between fluid and elastic structures in transient processes of hydraulic machines. However, very few published investigations are available in this regard.

### 3.3.3. Solution to unsteady boundary conditions

Unsteady boundary conditions at the inlet and outlet of hydraulic machines greatly influence the accuracy of 3-D simulation results in hydraulic machines [83,84]. Some researchers directly determine boundary conditions based on unsteady experimental data [19,27]. This treatment is relatively accurate; however, it relies on experimental tests. Besides, in prototype tests of transient processes, pressure measurements are easier to perform compared to direct measurement of unsteady discharge in hydraulic machines. Consequently, unsteady pressure boundary conditions are usually set at the inlet and outlet of hydraulic machines instead of discharge boundary conditions. Meanwhile, total pressures are usually approximately replaced by static pressures at the inlet [85]. This approximation obviously causes a certain degree of deviation in transient simulation results.

### 3.3.4. Solution to turbulent-flow simulations

During transient processes, severe turbulent flows exist within hydraulic machines. The severity of turbulent flows in hydraulic machines influences the accuracy of transient-flow simulations up to a certain degree [78]. Till date, in most transient-process simulations, 3-D transient flows in hydraulic machines are solved using the unsteady RANS method, wherein turbulent flows are modeled using all kinds of turbulence models— $k-\epsilon$ , shear stress transport (SST),  $v^2 - f$  [86], scale-adaptive simulation (SAS) [87], and detached eddy simulation (DES) models [88]. Relevant researches suggest that simulation results obtained using the RANS method are not accurate enough [16,21,27,56]. Therefore, the more rigorous LES method must be adopted to simulate unsteady turbulent flows.

## 3.4. Coupled 1-D–3-D simulation of transient flows

### 3.4.1. Rationale behind coupled 1-D–3-D simulations

As already mentioned, 1-D simulation methods could not accurately simulate fluctuating nonlinear characteristics of transient processes, whereas 3-D simulations of the entire water-conveyance system use up substantial computational resources, and 3-D simulations of hydraulic machines depend heavily on experimental data. To overcome these shortcomings, a coupled 1-D–3-D simulation method was proposed to simulate interactions between transient flows in pipeline system and unsteady turbulent flows within hydraulic machines [84,89–91]. In

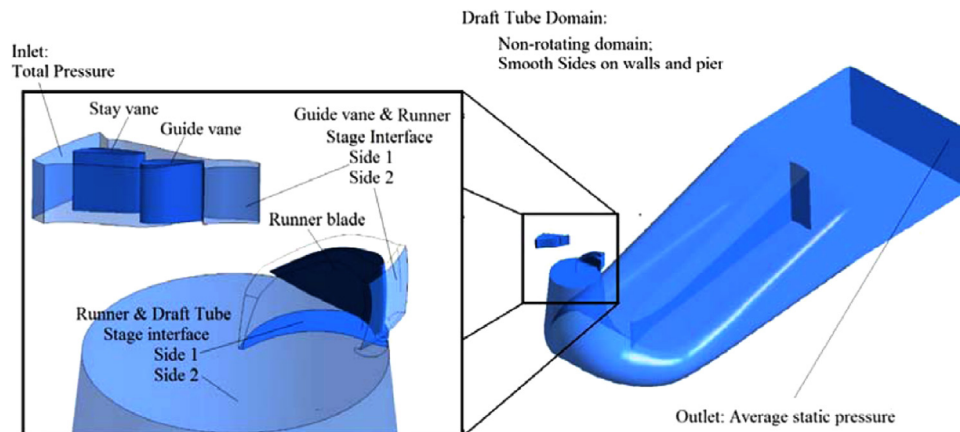


Fig. 19. Connection interface between any two adjacent parts [79].

coupled 1-D–3-D simulations (refer Fig. 20), transient flow in water-conveyance pipelines is simulated by adopting 1-D MOC, whereas the rather interesting unsteady turbulent flows in hydraulic machines are simulated by adopting the 3-D simulation method [60,61,92]. If the fluctuating free surface between water and air in the surge or tailrace is to be investigated [64,93,94], it could also be simulated using the 3-D method.

3.4.2. Methods for data exchange between 1-D and 3-D computational domains

In coupled 1-D–3-D simulations, use of reasonable methods for data exchange at the coupled 1-D–3-D boundary are vital for accurately simulating interactions between complex water-hammer phenomena in pipelines and unsteady turbulent flows within hydraulic machines. The following data-exchange methods have been used at the coupled 1-D–3-D boundary till date. Simple 1-D MOC and 3-D CFD coupled grids arrangements, as depicted in Fig. 21, are considered to illustrate data-exchange techniques.

In Fig. 21(a), the compatibility equation  $C^+$  could easily be constructed between S and  $P^{(n+1)}$  and expressed as

$$C^+: H_p^{(n+1)} = H_s^{(n)} - B(Q_p^{(n+1)} - Q_s^{(n)}) \tag{19}$$

To obtain an auxiliary equation to solve for  $H_p^{(n+1)}$  and  $Q_p^{(n+1)}$ ,  $H_p^{(n+1)}$  was substituted with  $H_{1-1}^{(n)}$ , in the earliest data-exchange method presented by Ruprecht et al. [84]. This method is relatively simple to formulate and program, and it effectively models the influence of water-hammer waves in a pipe system on the discharge at the 3-D CFD boundary. However, it involves the assumption  $H_p^{(n+1)} = H_{1-1}^{(n)}$ , which may not be valid if the difference in heads between adjacent time steps varies significantly [83]. The time step must, therefore, be sufficiently small. To overcome this shortcoming of the above data-exchange method, an improved method was proposed. During simulations, iteration results concerning the 1-D MOC and 3-D CFD methods were corrected with respect to each other, as depicted in Fig. 22 [95].

Both above-mentioned data-exchange methods possess rigorous theoretical bases. However, they are also quite complex, and researchers have not thoroughly discussed the convergences and accuracies of these methods. Later, Zhang and Cheng presented two explicit methods for data exchange at the coupled 1-D–3-D boundary [83,92], and efficiencies and accuracies of these methods were verified by simulating a water hammer within a pipeline system along with oscillating water levels within the surge tank. One of the two data exchange methods is the partly overlapped coupled method (POC) [83]. Its fundamental principle is depicted in Fig. 21(b). The downstream point M in the 1-D MOC grid boundary is located in Section 2–2 within the CFD grid. It is, therefore, referred to as the POC method. In Fig. 21(b), the compatibility equation  $C^+$  could still be easily constructed between S and  $P^{(n+1)}$ . However, different from the method of Ruprecht et al., in the POC method, another compatibility equation C<sup>-</sup> could easily be constructed between  $P^{(n+1)}$  and M.

$$C^-: H_p^{(n+1)} = H_M^{(n)} + B(Q_p^{(n+1)} - Q_M^{(n)}) \tag{20}$$

In this method,  $Q_M^{(n)}$  could be obtained based on calculation results of 3-D CFD during the nth time step, and calculation results ( $Q_p^{(n+1)}$ ) of 1-D MOC could be used as the inlet boundary condition of 3-D CFD during the (n + 1)th time step. This method models a section of the MOC grid using the CFD grid. Its physical meaning is relatively clear,

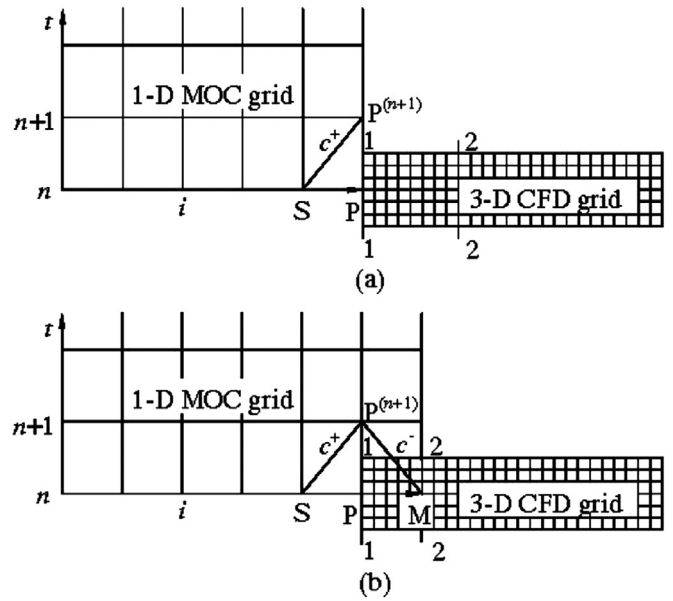


Fig. 21. Schematic of coupled 1-D–3-D grid arrangement [83].

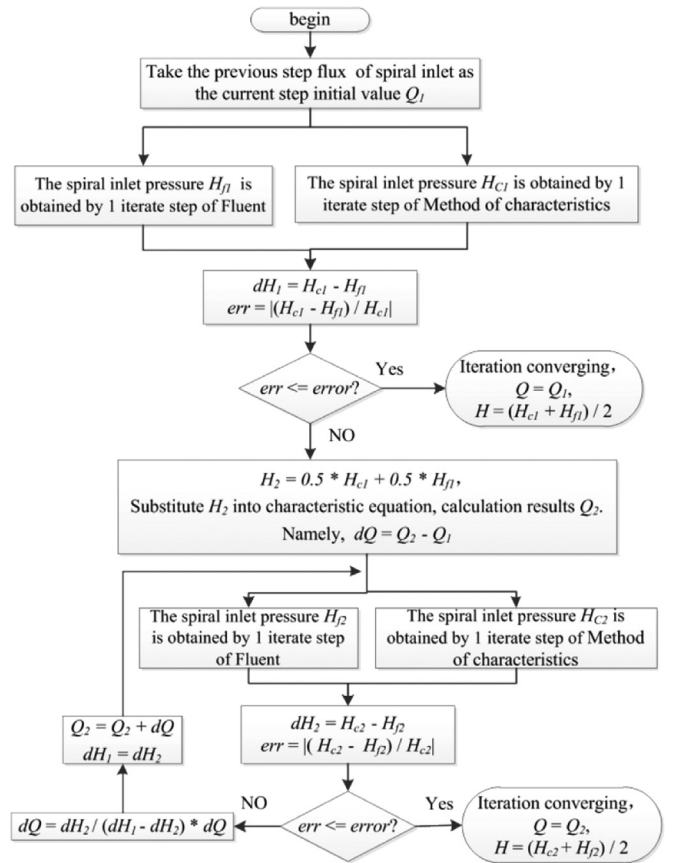


Fig. 22. Improved coupled 1-D–3-D coupled method [95].

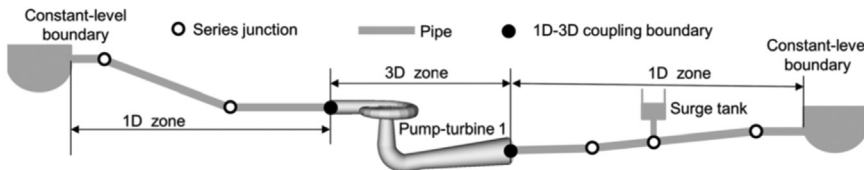


Fig. 20. Schematic of coupled 1-D–3-D simulation of pumped-storage power station [21].

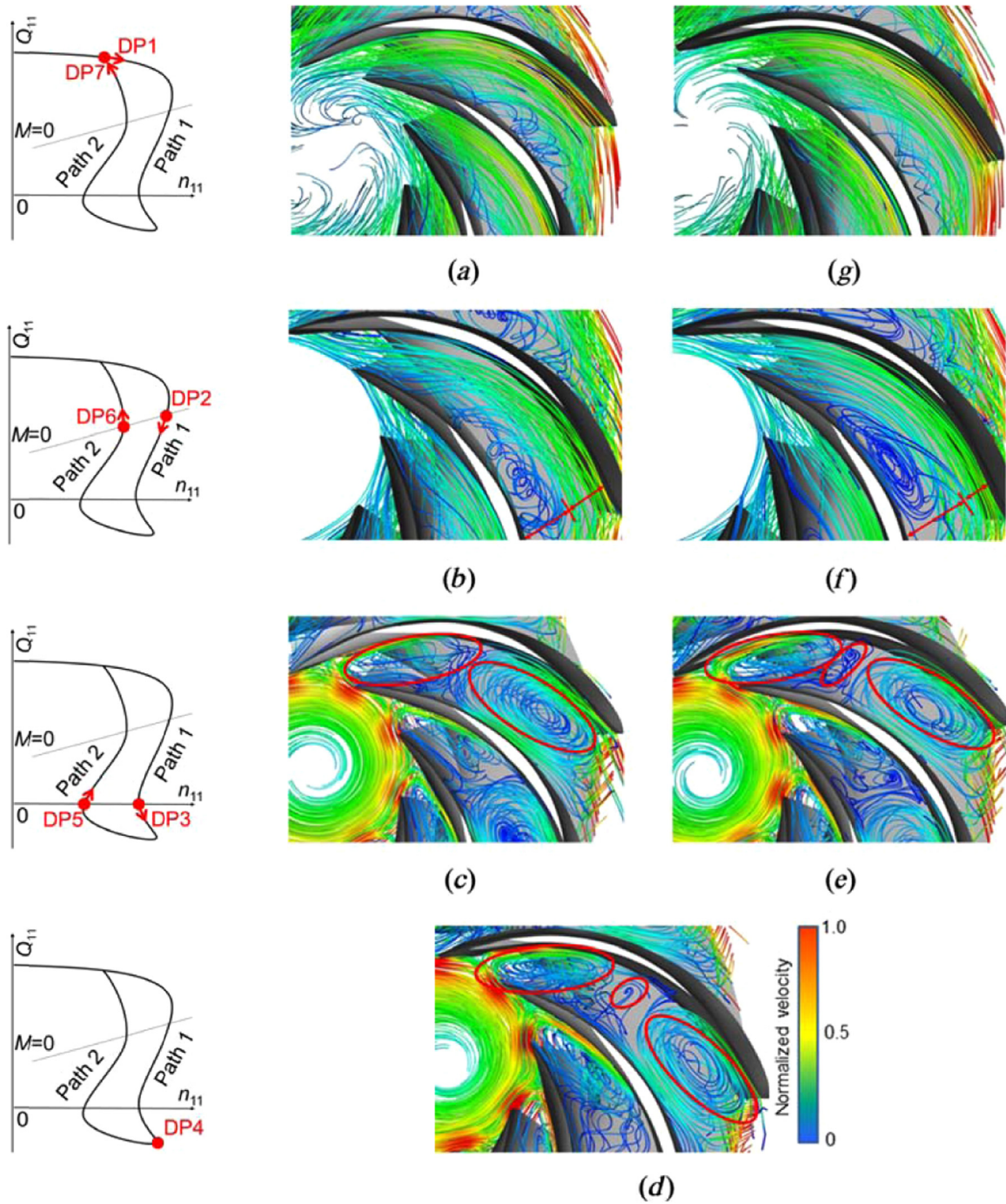


Fig. 23. Looping dynamic characteristics and flow mechanisms [21].

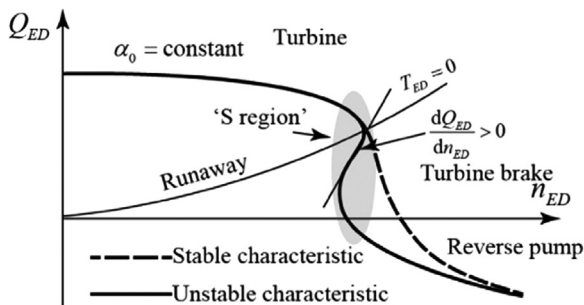


Fig. 24. S-shaped characteristics of pump-turbines [23].

and the corresponding procedure is also simple.

Another explicit data-exchange method is the adjacent coupling (AC) method [83]. Its fundamental principle is depicted in Fig. 21(a). Since the 1-D and 3-D grids are adjacent to each other, the method is referred to as the AC method. This method is similar to that of Ruprecht with respect to the arrangement of the grids in the two parts. However, no assumptions are made here. The additional relationship between  $H_p^{(n+1)}$  and  $Q_p^{(n+1)}$  could be deduced using the unsteady Bernoulli equation.

$$Q_{1-1}^{(n+1)} = Q_{1-1}^{(n)} + \Delta t \frac{gA}{h_{1-2}} [H_{1-1}^{(n)} - H_{2-2}^{(n)}] \quad (21)$$

Here,  $H_p^{(n+1)} = H_{1-1}^{(n+1)}$ ;  $Q_p^{(n+1)} = Q_{1-1}^{(n+1)}$ . This method has a more

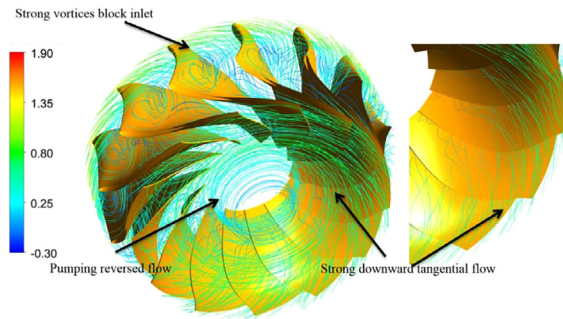


Fig. 25. Reverse flow and other unstable flow vortex structures near runner inlet and within draft tube represented using non-dimensional streamlines [79].

explicit physical meaning. However, the procedure is slightly more complex compared to the POC method. In addition, in analogy with the fluid–structure interaction methods, it is feasible to exchange data at the coupled 1-D–3-D boundaries based on the coupled MpCCI code.

### 3.4.3. Solution for compressibility of water

In previous 3-D transient flow simulations, water has always been considered an incompressible fluid. This simplification is reasonable in most cases [96,97], but is not suitable when simulating the water-hammer phenomenon, which takes into account the compressibility of

water in hydraulic machines during transient processes [98,99]. The unphysical incompressibility assumption, in this case, results in errors during transient simulations. For example, overpressure due to a sudden closing of the valve would be far greater compared to that observed in an actual case. Therefore, the compressibility of water must always be accounted for. Till date, two main methods have been used to simulate the weak compressibility of water in hydraulic machines during transient processes. One method is to define a density function (DDF) based on the following state equation of water and formula for acoustic speed of water within a pipe [83].

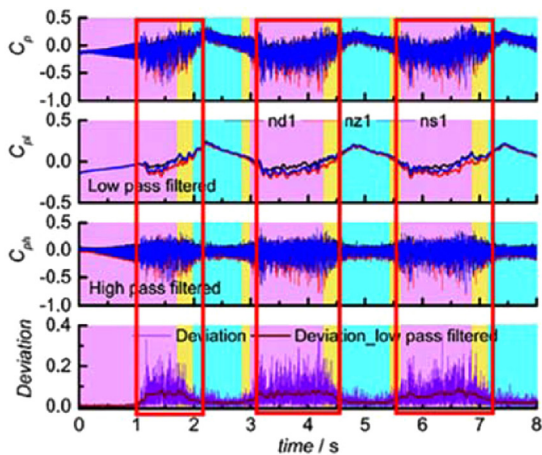
$$\frac{d\rho}{dP} = \frac{\rho}{K} \tag{22}$$

$$a^2 = \frac{\frac{K}{\rho}}{1 + c\frac{KD}{E}} \tag{23}$$

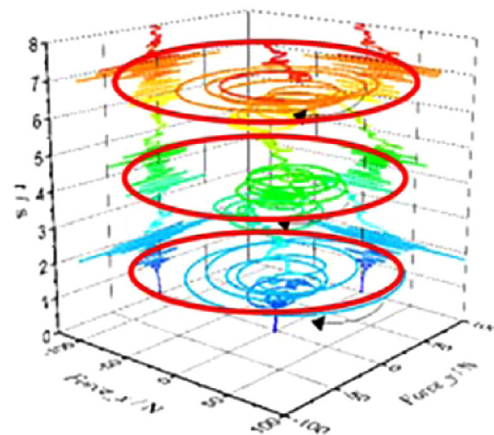
After mathematical treatment and simplification, the density of compressible water could be obtained using the following relation.

$$\rho = \rho_0 e^{(p-p_0)/\rho_0 a_0^2} \tag{24}$$

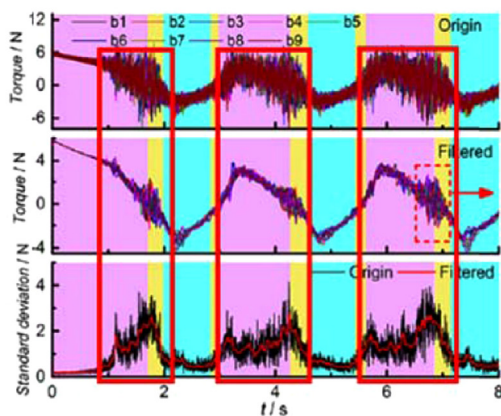
This method has a definite physical meaning. However, it is an explicit scheme, which means that the time step must be small enough to maintain accuracy. Another method is the modifying-the-ideal-gas-law (MIGL) method [83], which is relatively simple, and only requires modification of several parameters in the ideal gas law model for a



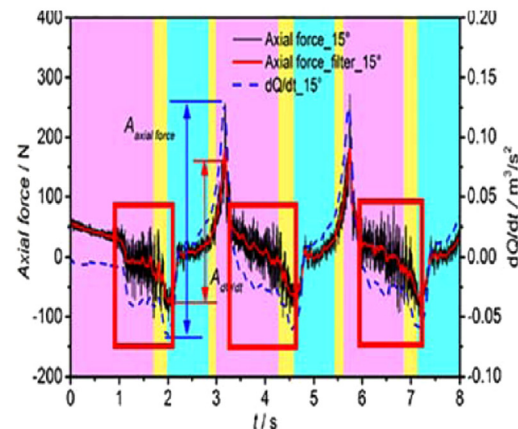
(a) pressure in vane-less space



(b) radial hydraulic thrusts on runner



(c) hydraulic torque on runner



(d) axial hydraulic thrust on runner

Turbine mode  Turbine breaking mode  Reverse pump mode

Fig. 26. Fluctuations in hydraulic exciting forces on runner during runaway [22].

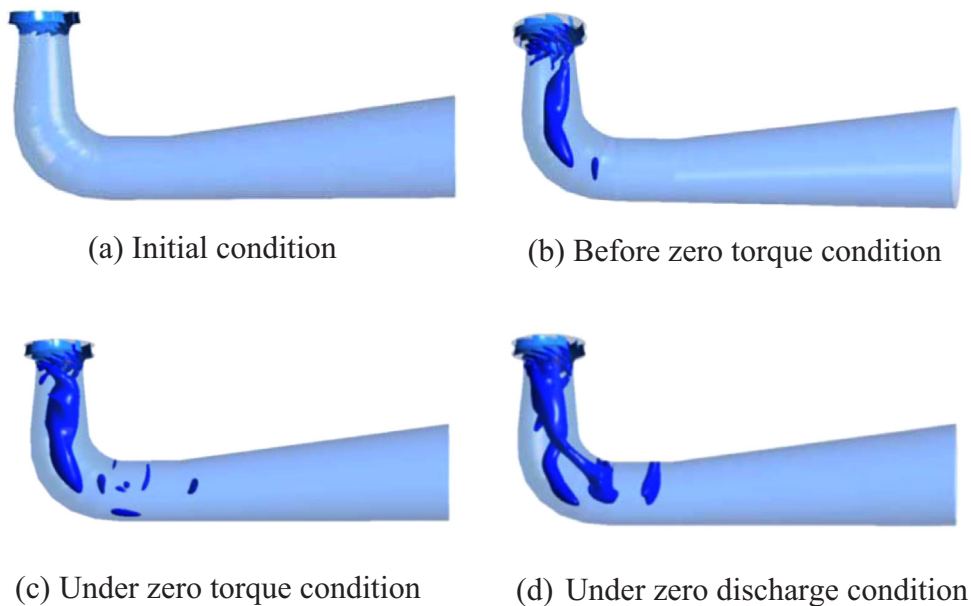


Fig. 27. Vortex rope within draft tube during load-rejection process [105].

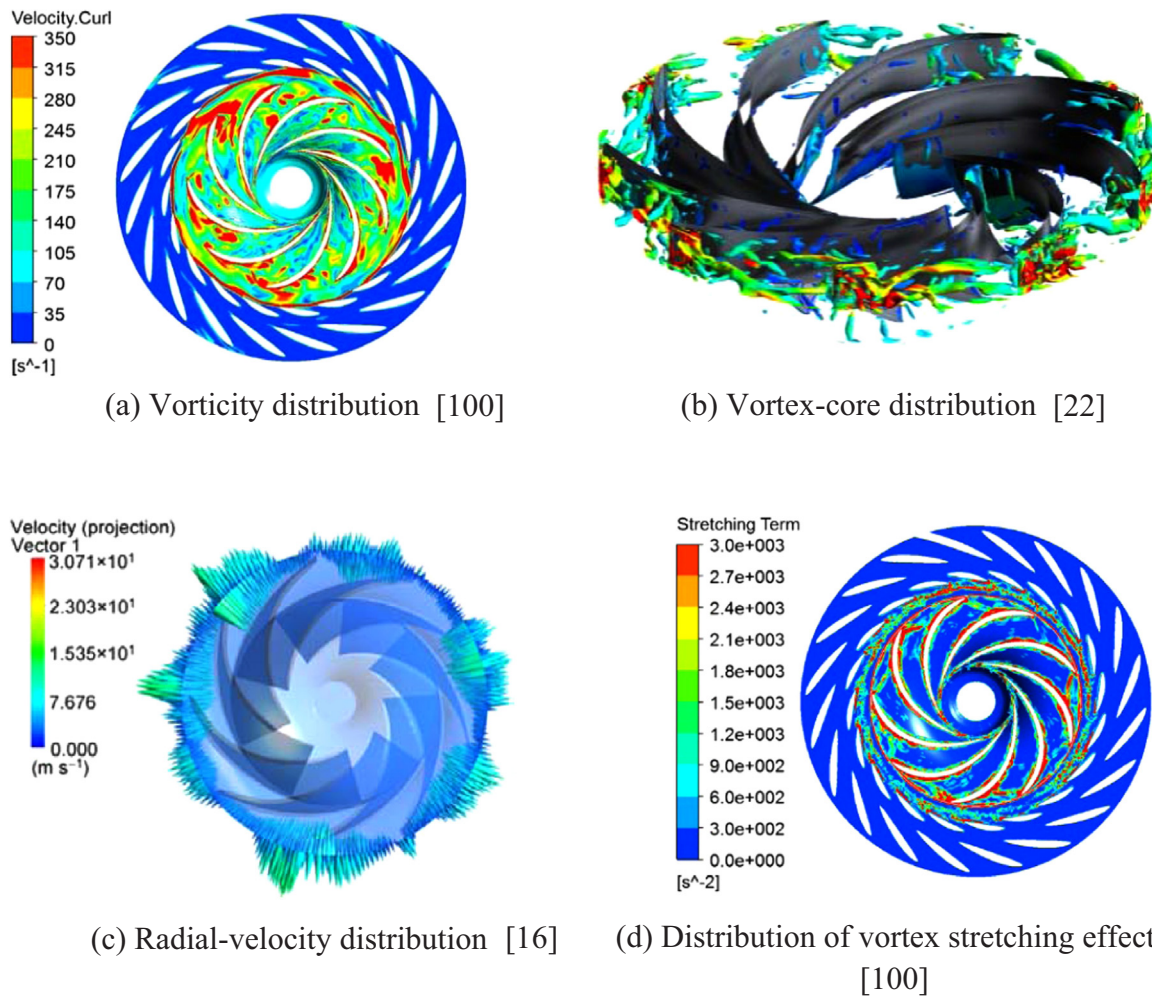


Fig. 28. Reverse flow vortex structures and corresponding formation mechanisms near runner inlets or vaneless spaces under no-load conditions.

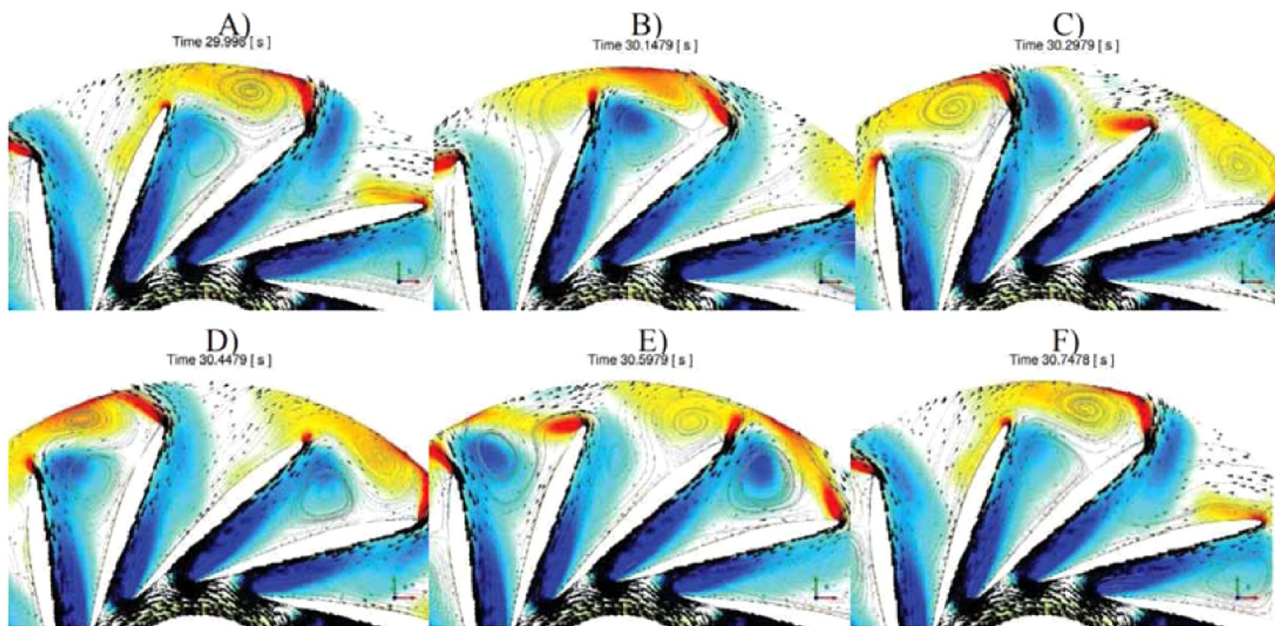


Fig. 29. Rotating stall at runner leading edge coloured by Z-component of vorticity (red: counter-clockwise rotating; blue: clockwise rotating) within a Francis turbine [73] (For interpretation of the references to color in this figure legend, the reader is referred to the web version of this article.).

compressible gas. However, it is unreliable in terms of its physical implications. Meanwhile, this method is also an explicit scheme. Additionally, it must be solved in conjunction with the energy equation, thereby consuming more computational resources compared to DDF.

#### 4. Transient characteristics and unsteady unstable flows investigations

During transient processes, hydraulic machines frequently switch operating modes between the turbine, brake, pump, and reverse-pump modes, as depicted in Fig. 1. Transient flow within water-conveyance pipeline systems interacts with the unsteady turbulent flow in hydraulic machines. Therefore, transient characteristics and flow patterns of transitions in hydraulic machines are very complex [100]. Based on previous experimental and numerical simulation methods of transient processes, some research results concerning transient characteristics and unsteady unstable flows within hydraulic machines during transient processes have been obtained as follows.

##### 4.1. Several transient characteristics and corresponding formation mechanisms

###### 4.1.1. Looping dynamic characteristics during runaway

Investigations have revealed that unit parameter curves dynamically loop in the S-shaped region during runaway; meanwhile, the transient rotational speed, discharge, and pressure oscillate with larger amplitudes, as depicted in Fig. 23 [21,39,80]. Zhang et al. [21,101] simulated and produced looping dynamic characteristics during the runaway process. Their numerical analysis suggests that this is caused by successive features of transient flow patterns. That is, transient flows within pump-turbines are influenced by their previous states, as depicted in Fig. 23.

###### 4.1.2. Instability of S-shaped curves during operating-mode transitions

Owing to hydraulic design defects, four quadrant characteristics of pump-turbines often demonstrate S-shaped characteristics, as depicted in Fig. 24. The S-shaped characteristics induce instabilities during transient processes of start-up, runaway, and load rejection in the turbine generating mode [16,39,102].

In accordance with the Rayleigh criterion, instabilities in hydraulic machines are closely related to instabilities concerning unsteady internal flows during transitions [20]. Further, related studies suggest that S-shaped instabilities are primarily caused by two physical mechanisms—the instantaneous impact of maximum reverse back-flow during operation in the reverse-pump mode and unsteady periodic motion of unstable flow patterns, such as reverse-flow vortex structures (RFVS) near runner inlets or vaneless spaces [16,27,87,103] and vortex ropes in draft tubes, as depicted in Fig. 25 [35,104,105].

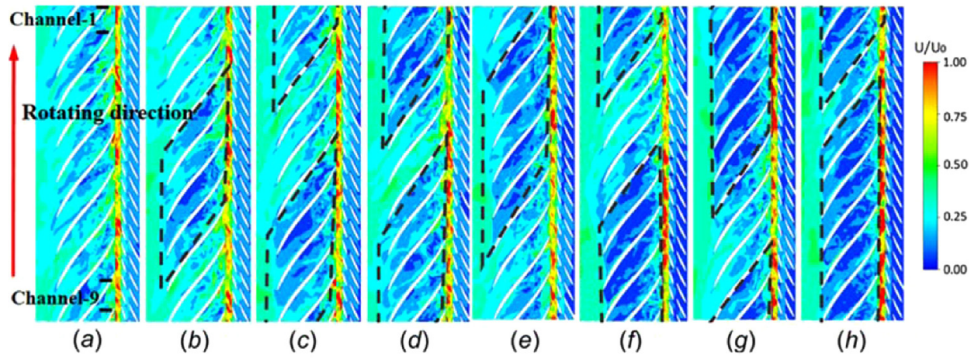
##### 4.1.3. Pulsating characteristics during transitions

During transient processes, the most direct and visible expressive forms of dynamic and unstable characteristics include the severe fluctuations of certain physical quantities. Especially, pressure fluctuations and fluctuations in hydraulic thrusts and torques on runners and guide vanes, as depicted in Fig. 26, are the ones more significant. These fluctuating hydraulic exciting forces and dynamic loads cause serious vibrations and noise within units and may even impact the fatigue life of runners. Additionally, they may even threaten the safety and stability of hydraulic-machine systems [106,107]. Related investigations suggest that severe fluctuations in pressure, radial hydraulic thrust on runners, and torques on guide vanes are primarily related to rotor-stator interactions and certain unsteady flow patterns, such as rotating stalls in hydraulic machines [80]. The severe fluctuations in axial hydraulic thrusts and torques on runners are mainly related to the reverse back-flow and unsteady vortex flows within draft tubes [22,106,107].

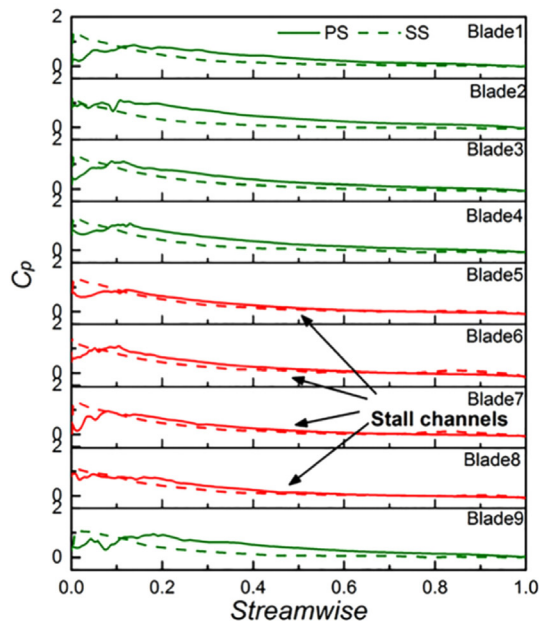
##### 4.2. Unstable unsteady flows and corresponding formation mechanisms

###### 4.2.1. Vortex ropes within draft tubes during transitions

A vortex rope within a draft tube is a general unstable unsteady flow. It usually occurs and mixes with cavitation flows. Its nature is still not fully understood. However, vortex ropes within draft tubes have been captured many times during transient processes [22,60,105,108,109]. According to research results reported by Liu et al. [105,110], during a load-rejection process, vortex ropes in draft tubes rotate in the same direction as the runner. This occurs before pump-turbines run at the zero torque (speed no-load condition) point. Additionally, a vortex rope can be divided into two parts as the flow



(a) Rotating stall flow patterns at mid-span section of runner/guide vane in pump–turbine at representative instants—(a)  $t=56.54$  s, (b)  $t=56.60$  s, (c)  $t=56.66$  s, (d)  $t=56.72$  s, (e)  $t=56.78$  s, (f)  $t=56.84$  s, (g)  $t=56.90$  s, and (h)  $t=56.96$  s [22].



(b) Asymmetrical pressure distribution on runner blades caused by rotating stall [22].

Fig. 30. Rotating stall and its effects on pump–turbine operation.

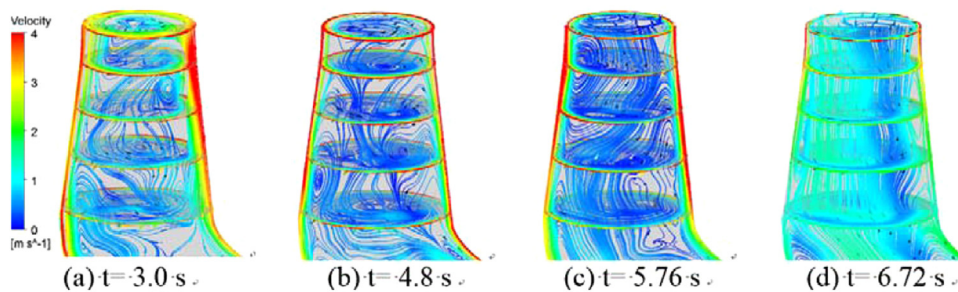


Fig. 31. Reverse back-flow within draft tubes at four typical instants during load-rejection process [106].

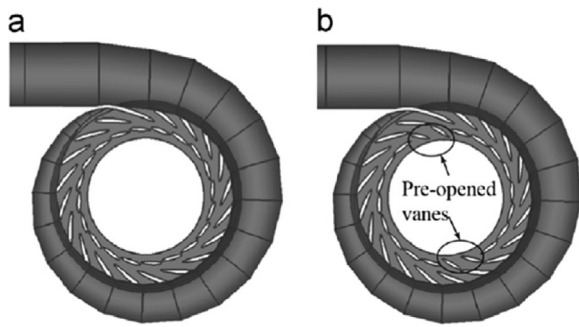


Fig. 32. Two opening guide-vane schemes—(a) synchronous guide vanes; (b) misaligned guide vanes (MGV) [2].

rate decreases to zero, as depicted in Fig. 27.

4.2.2. Reverse-flow vortex structures near runner inlet or within vaneless space

Many investigations have revealed the existence of unsteady, unstable flow vortex structures near runner inlets or within the vaneless space during transient processes [22,100], as depicted in Fig. 28(a)–(b). These unstable flow vortex structures tend to block runner inlets and influence energy transformations [79,103]. Consequently, they affect the stability of hydraulic-machine systems. Further investigations have reported that local unstable flow vortex structures near runner inlets demonstrate reverse flow under zero torque conditions (speed no-load

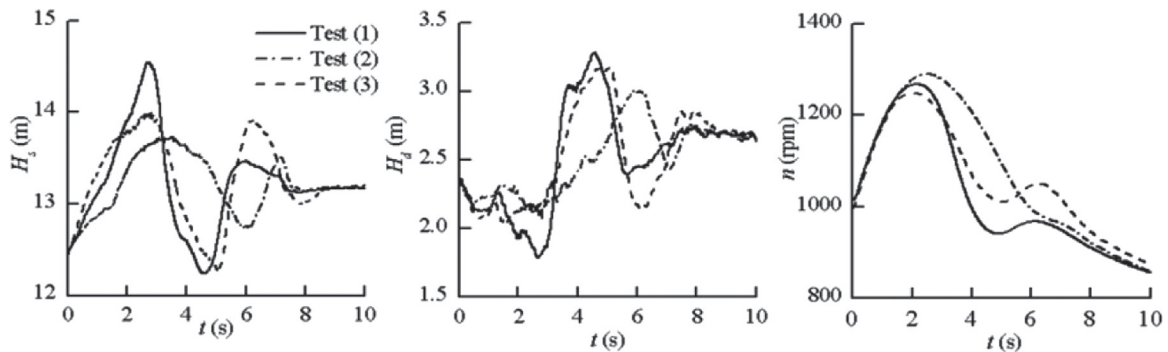
condition) [16,22], as depicted in Fig. 28 (c). They are, therefore, referred to as RFVS (Reverse-flow vortex structure). These unstable flow vortices develop from primary vortex cores under the action of stretching, bending, and twisting phenomena, as depicted in Fig. 28 (d) [100]. The primary vortex cores are mainly flow separation vortices that exist near leading edges of runner blades and those near the solid walls of the cover and bottom ring.

4.2.3. Rotating stall within runner

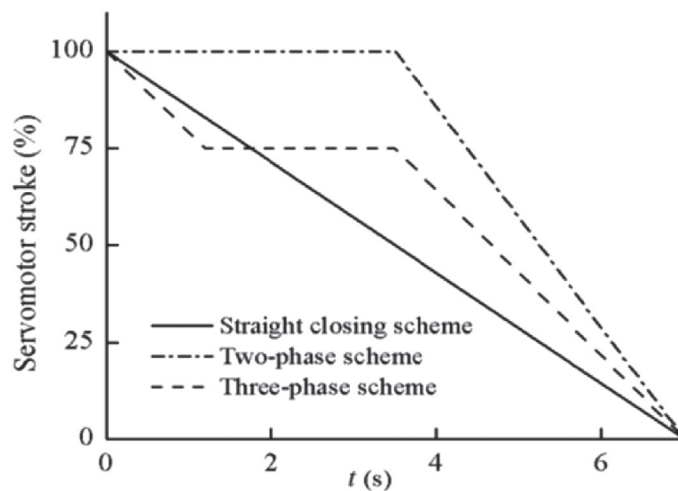
Rotating stalls within runners are unstable flow vortices that exist within runner channels. During transient processes, this unstable flow phenomenon, as shown in Fig. 29, has also been captured and reported in numerous investigations [20,22,73,86,110]. It generally occurs under lower discharge conditions and is closely related to the flow-separation vortex. The stall vortices propagate at a speed lower compared to the rotating speed of the runner. Therefore, propagating stall vortices are called rotating stalls. Evolving rotating stalls induce partial blockages within runner channels and asymmetrical pressure distributions on runner blades. Consequently, they cause intense fluctuations of hydraulic torques and radial forces on the runner, as depicted in Fig. 30 [22].

4.2.4. Reverse back-flow

Owing to frequent changes in operating modes and flow-pattern transitions, reverse back-flows often occur in hydraulic machines during transient processes, such as RFVS near runner inlets and local reverse back-flows that occur near draft tube inlets [79,106,111], as



(a) Variations in measured transient parameters when using different guide-vane closing schemes [115].



(b) Comparison of three different guide-vane closure schemes [115].

Fig. 33. Three different guide-vane closure schemes and corresponding transient parameter trends during transitions.

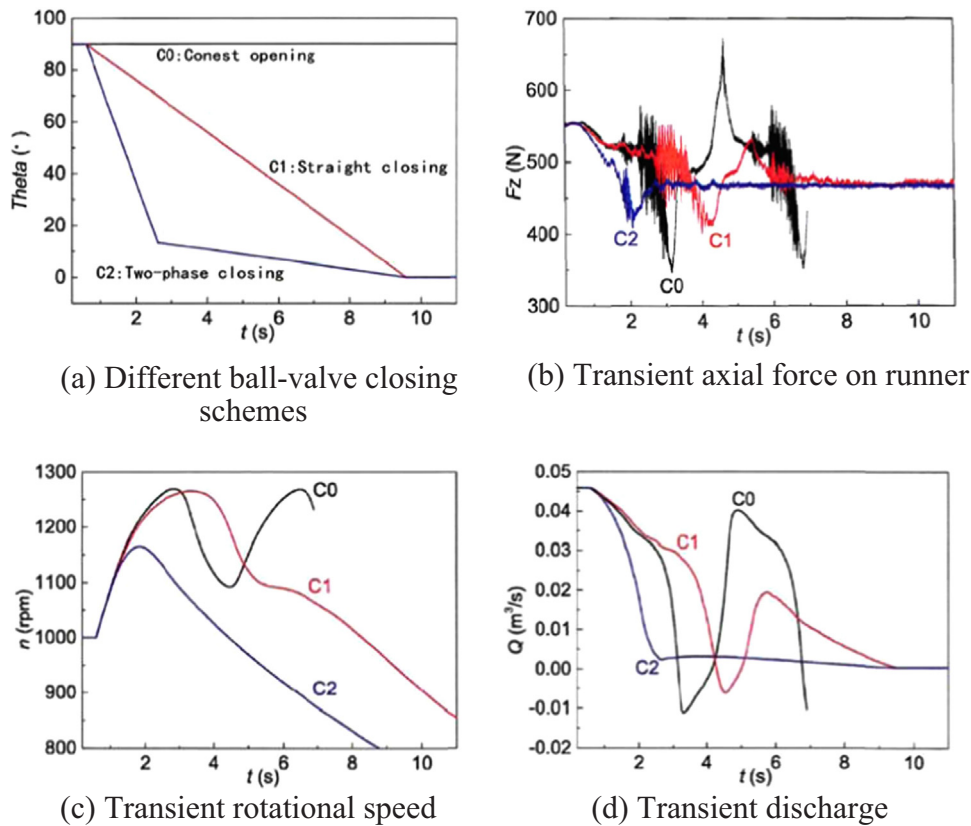


Fig. 34. Different ball-valve closing schemes and corresponding transient parameters during transitions [17].

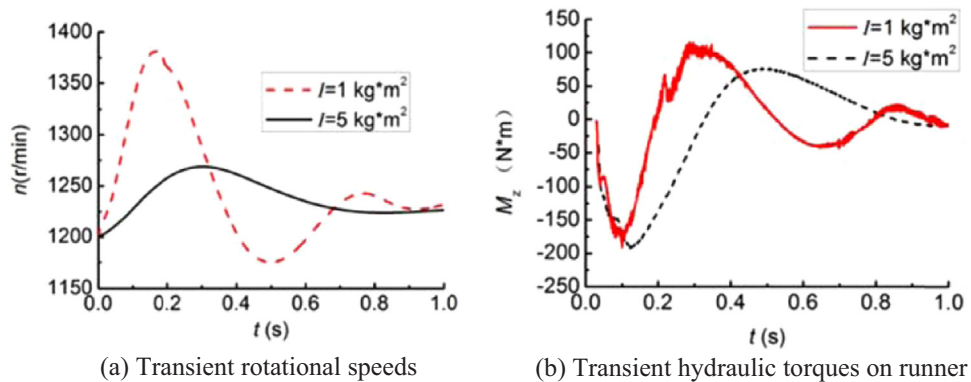


Fig. 35. Different moments of inertia and corresponding transient parameters during mode transitions [20].

depicted in Fig. 31. The effects of reverse back-flows are also very significant. In particular, during reverse-pump operating mode and the process of vapour-cavity collapse within a draft tube, the instantaneous impact of large reverse back-flows and reverse water hammers is quite significant. Such impacts induce intensive fluctuations and vibrations within hydraulic machines and may even affect their fatigue life [27,67].

**5. Notable issues concerning design and operation of hydraulic-machine systems**

Transient processes are rather complex, and many questions regarding transient processes and research methods yet remain unanswered. However, as regard actual engineering applications, certain notable issues concerning design and operation of hydraulic machines can be identified as follow.

**5.1. Opening and closing schemes for valves and guide vanes and their influence on system operation**

In accordance with theories, simulations, and experiments performed concerning transitions that occur within hydraulic-machine systems, it is possible to improve the stability and eliminate unstable flows within hydraulic-machine systems during transitions by changing the opening and closing schemes of valves and guide vanes [31,32,40,112]. Related research progresses could be summarized as under.

**5.1.1. Opening scheme for guide vanes and its influence**

As regards the opening scheme of guide vanes, related investigations suggest that preopening suitable misaligned guide vanes (MGV), as depicted in Fig. 32, can eliminate the manifestation of unstable S-shaped characteristics during start-up [108,113]. However, MGVs tend to destroy flow-field symmetry within pump-turbines. Furthermore,

they can induce and aggravate fluctuation characteristics [108,114].

### 5.1.2. Closing schemes of guide vanes and its influence

With regard to the closing scheme of guide vanes, Fan et al. [107] analysed the effects of the guide-vane closure law on flow patterns developed within guide-vane passages along with the hydraulic torque on a single guide vane. Their results indicate that use of a suitable guide-vane closure law could reduce unstable flows and hydraulic torque fluctuations within guide vanes. In addition, Zeng et al. [39,115] theoretically analysed principles of improving closing schemes of guide vanes based on transient characteristics within the S-shaped region, and proposed a selection method based on a two-phase closing scheme of guide vane. Analysis results demonstrate the advantages of three-phase guide-vane closing schemes in terms of controlling pulsating pressures and runaway speeds, as depicted in Fig. 33.

### 5.1.3. Opening and closing schemes of valves and their influence

With regard to opening and closing schemes for ball valves, Hua [116] validated 3-D simulations concerning ball-valve closure. Based on previous research, You [17] numerically investigated the effects of different ball-valve closure schemes on fluctuations and reverse back-flows within a pump–turbine. Compared with the linear closing scheme of a ball valve, the two-phase ball-valve closing scheme is recommended to eliminate servomotor failure of guide vanes, as depicted in Fig. 34.

## 5.2. Inertia of hydraulic unit and its influence

Liu et al. [20] numerically investigated the effects of inertia on operational stability of a pump–turbine. Their results demonstrated that increases in inertia can greatly decrease transient runaway speeds whilst also reducing fluctuations in hydraulic torque on the runner, as depicted in Fig. 35(a)–(b). Owing to S-shaped instability, a pump–turbine must operate under the turbine, turbine braking, and reverse-pump modes during the start-up process. It is difficult for a pump–turbine to be synchronized if it runs into an unstable reverse-pump mode. When increases in inertia are sufficiently large, the characteristic curve circles in a very small region, and the pump–turbine could avoid switching over to the reverse-pump mode. However, any decreases in inertia would result in the pump–turbine easily running into reverse-pump operation. Therefore, inertia considerably affects the stability of a pump–turbine. Improvements to this case can be made by increasing the moment of inertia. In addition, stall phenomena within a runner could also be avoided by increasing the moment of inertia.

## 6. Conclusions

This paper presents a review of transition phenomena that occur within hydraulic-machine systems based on investigations reported extensively in relevant literature. In this review, the authors have summarized the findings of these investigations mainly with respect to experimental and numerical-simulation methods of analysing transitions, transient characteristics, unsteady unstable flows phenomena within hydraulic machines, and certain notable issues concerning the design and operation of hydraulic-machine systems.

Transient processes that occur within actual hydraulic-machines systems are extremely complex and are influenced by numerous factors, including occurrence of the water-hammer phenomena, cavitation, fluid–structure interactions, rotor–stator interactions, and interactions between transient flow within pipelines and turbulent flows within hydraulic machines. To accurately simulate the physical effects that manifest during specific transitions, a suitable simulation scenario must be flexibly established in accordance with simulation strategies described in this paper.

The complex transient characteristics of hydraulic-machine transitions, such as dynamic looping characteristics, S-shaped instabilities,

and fluctuation characteristics, are primarily caused by unsteady unstable flow patterns, including vortex ropes in draft tubes, reverse-flow vortex structures near runner inlets, rotating stalls in the runner passage, and reverse back-flows. To address the impact of these phenomena, effective countermeasures must be explored and considered in the design and operation of hydraulic-machine systems in addition to such techniques as changing the inertia, opening and closing schemes of guide vanes and valves, and so on.

According to our review of the literatures on transient processes in hydraulic machinery system, most previous studies use numerical simulations to investigate transitions. Experimental investigations of transient processes are very rare and valuable. Therefore, in the future, more experimental investigations on transient processes of hydraulic machinery system should be conducted.

## Acknowledgments

The authors would like to thank National Natural Science Foundation of China (Grant No. 51876047, Grant No. 51476083 and Grant No. 51806044), Open Research Fund Program of State key Laboratory of Hydrosience and Engineering, China (sklhse-2018-E-02), Open Fund of Key Laboratory of Fluid and Power Machinery (Xihua University), Ministry of Education Sichuan, China (Grant No. szjj-2017-100-1-001), Fundamental Research Funds for the Central Universities, China (Grant No. HIT. NSRIF. 2019063), China Postdoctoral Science Foundation (No. 2018M630353), and National Key Research and Development Program, China (Grant No. 2018YFB0905205) for their financial supports.

## Conflict of interests

The authors declare that there is no conflict of interests regarding the publication of this article.

## References

- [1] Liu X, Luo Y, Wang Z. A review on fatigue damage mechanism in hydro turbines. *Renew Sustain Energy Rev* 2016;54(2016):1–14.
- [2] Zuo Z, Liu S, Sun Y, et al. Pressure fluctuations in the vaneless space of high-head pump-turbines—a review. *Renew Sustain Energy Rev* 2015;41(2015):965–74.
- [3] Yang J, Xie T, Giorgio P, et al. Numerical study on rotating characteristics of unsteady flow inner pump-turbine in pump mode. *Int J Fluid Mach Syst* 2018;11(3):224–33.
- [4] Yang J, Pavesi G, Yuan S, et al. Experimental characterization of a pump–turbine in pump mode at hump instability region. *J Fluids Eng -Trans ASME* 2015;137(5):051109.
- [5] Luo XW, Yu A, Ji B, et al. Unsteady vortical flow simulation in a Francis turbine with special emphasis on vortex rope behavior and pressure fluctuation alleviation. *Proc Inst Mech Eng Part A J Power Energy* 2017;231(3):1–12.
- [6] Li D, Wang H, Qin Y, et al. Entropy production analysis of hysteresis characteristic of a pump-turbine model. *Energy Convers Manag* 2017;149:175–91.
- [7] Li D, Wang H, Qin Y, et al. Numerical simulation of hysteresis characteristic in the hump region of a pump-turbine model. *Renew Energy* 2018;115(2018):433–47.
- [8] Li D, Wang H, Qin Y, et al. Mechanism of high amplitude low frequency fluctuations in a pump-turbine in pump mode. *Renew Energy* 2018;126:668–80.
- [9] Zhang YN, Chen T, Li JW, et al. Experimental study of load variations on pressure fluctuations in a prototype reversible pump turbine in generating mode. *J Fluids Eng-Trans ASME* 2017;139(1):074501.
- [10] Yang J, Pavesi G, Liu X, et al. Unsteady flow characteristics regarding hump instability in the first stage of a multistage pump-turbine in pump mode. *Renew Energy* 2018;127:377–85.
- [11] Li X, Gao P, Zhu Z, et al. Effect of the blade loading distribution on hydrodynamic performance of a centrifugal pump with cylindrical blades. *J Mech Sci Technol* 2018;32(3):1161–70.
- [12] Li X, Jiang Z, Zhu Z, et al. Entropy generation analysis for the cavitating head-drop characteristic of a centrifugal pump. *Proc Inst Mech Eng Part C: J Mech Eng Sci* 2018. <https://doi.org/10.1177/0954406217753458> 163.
- [13] Tan L, Yu Z, Xu Y, et al. Role of blade rotational angle on energy performance and pressure fluctuation of a mixed-flow pump. *Proc Inst Mech Eng Part A: J Power Energy* 2017;231(3):227–38.
- [14] Zuo Z, Fan H, Liu S, et al. S-shaped characteristics on the performance curves of pump-turbines in turbine mode – a review. *Renew Sustain Energy Rev* 2016;60(2016):836–51.
- [15] Zhang H, Chen D, Wu C, et al. Dynamic modeling and dynamical analysis of pump-turbines in S-shaped regions during runaway operation. *Energy Convers Manag*

- 2017;138:375–82.
- [16] Yin J, Wang D, Walters K, et al. Investigation of the unstable flow phenomenon in a pump turbine. *Sci China Phys Mech Astron* 2014;57(6):1119–27.
- [17] You J. Cavitation characteristics and transient processes of a pump-turbine analyzed by three-dimensional simulation. Wuhan University; 2017. [in Chinese].
- [18] Li Z, Bi HL, Wang Z, et al. Three-dimensional simulation of unsteady flows in a pump-turbine during start-up transient up to speed no-load condition in generating mode. *Proc Inst Mech Eng Part A J Power Energy* 2016;230(6):570–85.
- [19] Li Z, Bi H, Karney B, et al. Three-dimensional transient simulation of a prototype pump-turbine during normal turbine shutdown. *J Hydraul Res* 2017;55(4):520–37.
- [20] Liu J, Liu S, Sun Y, et al. Instability study of a pump-turbine at no load opening based on turbulence model. *IOP Conf Ser: Earth Environ Sci* 2012;15(7):2035.
- [21] Zhang X, Cheng Y, Xia L, et al. Looping dynamic characteristics of a pump-turbine in the s-shaped region during runaway. *J Fluids Eng-Trans ASME* 2016;138(9):091102.
- [22] Xia L, Cheng Y, Yang Z, et al. Evolutions of pressure fluctuations and runner loads during runaway processes of a pump-turbine. *J Fluids Eng-Trans ASME* 2017;139(9):091101.
- [23] International Electrotechnical Commission. IEC 60193 hydraulic turbines, storage pumps and pump-turbines: model acceptance tests. Geneva; 1999.
- [24] International Electrotechnical Commission. IEC 41 field acceptance tests to determine the hydraulic performance of hydraulic turbines, storage pumps and pump-turbines. Geneva; 1991.
- [25] J. Hu, W. Zeng, J. Yang, et al. Transient pressure pulsations of a model pump-turbine during power failure. In: Proceedings of the ASME 2017 fluids engineering division summer meeting, Jul 30-Aug 3, Hilton Waikoloa Village, Waikoloa, Hawaii; 2017.
- [26] Trivedi C, Agnalt E, Dahlhaug A. Experimental investigation of a Francis turbine during exigent ramping and transition into total load rejection. *J Hydraul Eng* 2018;144(6):4018027.
- [27] Fu X, Li D, Wang H, et al. Dynamic instability of a pump-turbine in load rejection transient process. *Sci China Technol Sci* 2018. <https://doi.org/10.1007/s11431-017-9209-9>.
- [28] Trivedi C, Cervantes MJ, Bhupendrakumar G, et al. Pressure measurements on a high-head Francis turbine during load acceptance and rejection. *J Hydraul Res* 2014;52(2):283–97.
- [29] Trivedi C, Cervantes M, Gandhi B, et al. Transient pressure measurements on a high head model Francis turbine during emergency shutdown, total load rejection, and runaway. *ASME J Fluids Eng* 2014;136(12):1–18.
- [30] Trivedi C, Cervantes M, Gandhi B. Investigation of a high head Francis turbine at runaway operating conditions. *Energies* 2016;9(3):149.
- [31] Trivedi C, Gandhi B, Michel CJ. Effect of transients on Francis turbine runner life: a review. *J Hydraul Res* 2013;51(2):121–32.
- [32] Trivedi C, Gandhi BK, Cervantes MJ, et al. Experimental investigations of a model Francis turbine during shutdown at synchronous speed. *Renew Energy* 2015;83:828–36.
- [33] Gagnon M, Tahan SA, Bocher P, et al. Impact of startup scheme on Francis runner life expectancy. *IOP Conf Ser: Earth Environ Sci* 2010;12:12107.
- [34] Sun Y, Liu S, Liu J, et al. Experimental study of pressure pulsation of a pump-turbine in starting. *J Eng Thermophys* 2012;33(8):1330–3. [in Chinese].
- [35] Amiri K, Mulu B, Raisee M, et al. Unsteady pressure measurements on the runner of a Kaplan turbine during load acceptance and load rejection. *J Hydraul Res* 2016;54(1):1–18.
- [36] Houde S, Fraser R, Ciocan G, et al. Experimental study of the pressure fluctuations on propeller turbine runner blades: part 2, transient conditions. *IOP Conf Ser: Earth Environ Sci* 2012;15(6):62061.
- [37] Yang J, Hu J, Zeng W, et al. Transient pressure pulsations of prototype Francis pump-turbines. *J Hydraul Eng* 2016;147(7):858–64. [in Chinese].
- [38] N. Ruchonnet, O. Braun. Reduced scale model test of pump-turbine transition. In: Proceedings of the 6th IAHR international meeting of the workgroup on cavitation and dynamic problems in hydraulic machinery and systems, September 9–11, Ljubljana, Slovenia; 2015.
- [39] Zeng W, Yang J, Hu J, et al. Effects of pump-turbine S-shaped characteristics on transient behaviours: experimental investigation. *J Phys: Conf Ser* 2017;813(1):12056.
- [40] Li Z. Numerical simulation and experimental study on the transient flow in centrifugal pump during starting period. Zhejiang University; 2009. [in Chinese].
- [41] Wang F, Bai M, Xiao R. Analysis on hydraulic transients of pumping station with flowmaster. *J Drain Irrig Mach Eng* 2010;28(2):144–8.
- [42] Zhou J, Lai X, Tang L. A modeling approach for dynamic simulation of hydroelectric generating set with flowmaster. *China Rural Water Hydropower* 2008;2:102–4. [in Chinese].
- [43] Wang X. The calculation and analysis of hydraulic transients of Huanggou pumped storage hydroplant. Changchun Institute of Technology; 2015. [in Chinese].
- [44] Wang B. Study on transient process computing of water diversion system for pumped power station. Huazhong University of Science and Technology; 2012. [in Chinese].
- [45] Ghidaoui MS, Zhao M, Mcinnis DA, et al. A review of water hammer theory and practice. *Appl Mech Rev* 2005;58(1):49–76.
- [46] Walseth E, Nielsen T, Svingen B. Measuring the dynamic characteristics of a low specific speed pump-turbine model. *Energies* 2016;9(3):199.
- [47] Yang J. Study on the characteristics of pump-turbine and transient process based on the curved surface. Wuhan University; 2014. [in Chinese].
- [48] Liu Z, Zheng D, Liu Y, et al. New Suter-transformation method of complete characteristic curves of pump-turbines based On the 3-D surface. *China Rural Water Hydropower* 2015;1:143–57. [in Chinese].
- [49] Yang X. Deal on characteristic curves of pump-turbine and study on the regulating control of hydraulic transients. Huazhong University of Science and Technology; 2012. [in Chinese].
- [50] Chang J. Transients of hydraulic machine installations. Beijing: China Higher Education Press; 2005. [in Chinese].
- [51] Li YM, Song GQ, Yan YL. Transient hydrodynamic analysis of the transition process of bulb hydroelectric turbine. *Adv Eng Softw* 2015;90(2015):152–8.
- [52] Zhang L, Zhou D. CFD research on runaway transient of pumped storage power station caused by pumping power failure. *IOP Conf Ser: Mater Sci Eng* 2013;52(5):52027.
- [53] Zhou DQ, Zhang LG. Numerical test of the transition process of pumping power failure pump condition in a pumped storage power station. *J Huazhong Univ Sci Technol [Sci Technol]* 2014;42(2):16–20.
- [54] Li JW, Yu J, Wu YL. 3D unsteady turbulent simulations of transients of the Francis turbine. *IOP Conf Ser: Earth Environ Sci* 2010;12(1):12001.
- [55] X. Zhang, Y. Cheng. CFD simulation of 3D transients in bulb turbine. In: Proceedings of the national symposium on hydrodynamics and the 110th anniversary commemorative conference of Zhou Peiyuan's birthday; 2012.
- [56] Xia L, Cheng Y, Zhang X, et al. 3D CFD simulation of the runaway transients of bulb turbine. *J Sichuan Univ (Eng Sci Ed)* 2014;46(5):35–41.
- [57] Kolšek T, Duhovnik J, Bergant A. Simulation of unsteady flow and runner rotation during shut-down of an axial water turbine. *J Hydraul Res* 2006;44(1):129–37.
- [58] Luo X, Li W, Feng J, et al. Simulation of runaway transient characteristics of tubular turbine based on CFX secondary development. *Trans Chin Soc Agric Eng* 2017;33(13):97–103.
- [59] Li W. Numerical simulation of unsteady flow in transient process of Francis turbine units. Xi'an University of Technology; 2014. [in Chinese].
- [60] Cherny S, Chirkov D, Bannikov D, et al. 3D numerical simulation of transient processes in hydraulic turbines. *IOP Conf Ser: Earth Environ Sci* 2010;12(1):12071.
- [61] Avdyushenko AY, Cherny SG, Chirkov DV, et al. Numerical simulation of transient processes in hydroturbines. *Thermophys Aeromech* 2013;20(5):577–93.
- [62] Zhou DQ, Zhong LJ, Zheng Y, et al. Numerical simulation of transient flow in axial-flow pump unit model during runaway caused from power failure. *J Drain Irrig Mach Eng* 2012;30(4):401–6. [in Chinese].
- [63] Zhou D, Chen H, Zhang L, et al. Investigation of pumped storage hydropower power-off transient process using 3D numerical simulation based on SP-VOF hybrid model. *Energies* 2018;11(4):1–16.
- [64] Yuan Y, Fan H, Li F, et al. Study on three-dimensional flow in surge tank with consideration of pipeline property. *J Hydroelectr Eng* 2012;31(1):168–72. [in Chinese].
- [65] Meng L. The study of cavitation influence on centrifugal pump startup process. China Agricultural University; 2016. [in Chinese].
- [66] Panov LV, Chirkov DV, Cherny SG, et al. Numerical simulation of pulsation processes in hydraulic turbine based on 3D model of cavitating flow. *Thermophys Aeromech* 2014;21(1):31–43.
- [67] Zhang X, Cheng Y, Xia L, et al. CFD simulation of reverse water-hammer induced by collapse of draft-tube cavity in a model pump-turbine during runaway process. *IOP Conf Ser: Earth Environ Sci* 2016;49(2016):52017.
- [68] Pejovic S, Karney BW, Gajic A. Analysis of pump-turbine S instability and reverse waterhammer incidents in hydropower systems. *J Trauma* 2011;70(4):970–7.
- [69] Fu X, Li D, Wang H, et al. Influence of the clearance flow on the load rejection process in a pump-turbine. *Renew Energy* 2018;127:310–21.
- [70] Mao X, Monte AD, Benini E, et al. Numerical study on the internal flow field of a reversible turbine during continuous guide vane closing. *Energies* 2017;10(7):988.
- [71] Nicolle J, Morissette JF, Giroux AM. Transient CFD. Simulation of a Francis turbine startup. *IOP Conf Ser: Earth Environ Sci* 2012;15(6):062014.
- [72] Mao X, Pavesi G, Zheng Y. Francis-type reversible turbine field investigation during fast closure of wicket gates. *J Fluids Eng-Trans ASME* 2018;140(6):61103.
- [73] Nicolle J, Giroux A, Morissette J. CFD configurations for hydraulic turbine startup. *IOP Conf Ser: Earth Environ Sci* 2014;22(3):32021.
- [74] Hao D. Numerical simulation of self-propelled of "C" type swimming fish using the immersed boundary method. Kunming University of Science and Technology; 2013. [in Chinese].
- [75] Lin L. Study on the interaction between the rigid body and fluid using projected immersed boundary method. Kunming University of Science and Technology; 2013. [in Chinese].
- [76] Su S. Research on the flow around tandem cascade of Francis turbine using the immersed boundary method. Kunming University of Science and Technology; 2014. [in Chinese].
- [77] Li S, Cheng Y, Zhang C. 3-dimensional transient flow simulation of tubular turbine based on Ib-Lb. *J Huazhong Univ Sci Technol (Nat Sci Ed)* 2016;44(1):122–7.
- [78] Fu X, Li D, Wang H, et al. Energy analysis in a pump-turbine during the load rejection process. *ASME J Fluids Eng* 2018;140(10):101107.
- [79] Hosseinimaneh H, Devals C, Nennemann B, et al. A numerical study of Francis turbine operation at no-load condition. *J Fluids Eng* 2017;139(1):11104.
- [80] Casartelli E, Mangani L, Ryan O, et al. Application of transient CFD-procedures for S-shape computation in pump-turbines with and without FSI[J]. *IOP Conf Ser: Earth Environ Sci* 2016;49(4):42008.
- [81] Pei J. Investigations on fluid-structure interaction of unsteady flow-induced vibration and flow unsteadiness intensity of centrifugal pumps. Jiangsu University; 2013. [in Chinese].
- [82] Nennemann B, Morissette JF, Chamberlandlauron J, et al. Challenges in dynamic pressure and stress predictions at No-load operation in hydraulic turbines. *IOP Conf Ser: Earth Environ Sci* 2014;22(3):32055.

- [83] Zhang X, Cheng Y. Simulation of hydraulic transients in hydropower systems using the 1-D-3-D coupling approach. *J Hydrodyn Ser B* 2012;24(4):595–604.
- [84] A. Ruprecht, T. Helmrich, T. Aschenbrenner, et al. Simulation of vortex rope in a turbine draft tube. In: *Proceedings of the hydraulic machinery and systems 21st IAHR symposium, Lausanne, Switzerland; 2002*.
- [85] Fu X. Research on the load rejection transient process of pump-turbine. Harbin Institute of Technology; 2017. [in Chinese].
- [86] Liu J, Liu S, Sun Y, et al. Three-dimensional flow simulation of transient power interruption process of a prototype pump-turbine at pump mode. *J Mech Sci Technol* 2013;27(5):1305–12.
- [87] Xia L, Cheng Y, You J, et al. Mechanism of the S-shaped characteristics and the runaway instability of pump-turbines. *J Fluids Eng Trans ASME* 2017;139(3):031101.
- [88] Pavesi G, Cavazzini G, Ardizzon G. Numerical analysis of the transient behaviour of a variable speed pump-turbine during a pumping power reduction scenario. *Energies* 2016;9(7):534.
- [89] A. Ruprecht, T. Helmrich. Simulation of the water hammer in a hydro power plant caused by draft tube surge. Hawaii, USA; 2003. p. 2811–6.
- [90] Liu Q. Investigation on 1D/3D coupling simulation on pump system during transient process. Zhejiang University; 2013. [in Chinese].
- [91] Fan H, Huang W, Chen N. Transient simulation of turbine jointed with diversion penstock. *J Drain Irrig Mach Eng* 2012;30(6):695–9.
- [92] Zhang XX, Cheng YG, Yang JD, et al. Simulation of the load rejection transient process of a Francis turbine by using a 1-D-3-D coupling approach. *J Hydrodyn Ser B* 2014;26(5):715–24.
- [93] Cheng Y, Li J, Yang J. Free surface-pressurized flow in ceiling-sloping tailrace tunnel of hydropower plant: simulation by Vof model. *J Hydraul Res* 2007;45(1):88–99.
- [94] Liu J, Li Z, Wang L, et al. Numerical simulation of the transient flow in a radial flow pump during stopping period. *J Fluids Eng-Trans ASME* 2011;133(11):111101.
- [95] Huang W, Fan H, Chen N. Transient simulation of hydropower station with consideration of three-dimensional unsteady flow in turbine. *IOP Conf Ser: Earth Environ Sci* 2012;15(5):52003.
- [96] J.L. Yin, D.Z. Wang, L.Q. Wang, et al. Effects of water compressibility on the pressure fluctuation prediction in pump turbine. In: *Proceedings of the 26th IAHR symposium on hydraulic machinery and systems; 2013*.
- [97] J. Yang, J. Koutnik, U. Seidel, et al. Compressible simulation of rotor-stator interaction in pump-turbines; 2010. p. 12008.
- [98] Yang S. Investigation on the transient characteristics of the pump system using MOC-CFD coupling method. Zhejiang University; 2015. [in Chinese].
- [99] Yin J. Study on the internal flow and optimum design of pump turbine in the "S" zone. Zhejiang University; 2012. [in Chinese].
- [100] Fu X, Li D, Wang H, et al. Analysis of transient flow in a pump-turbine during the load rejection process. *J Mech Sci Technol* 2018;32(5):2069–78.
- [101] Zhang X, Cheng Y, Xia L, et al. Dynamic characteristics of a pump-turbine during hydraulic transients of a model pumped-storage system: 3D CFD simulation. *IOP Conf Ser: Earth Environ Sci* 22. 2014. p. 32030.
- [102] Zeng W, Yang J, Guo W. Runaway instability of pump-turbines in S-shaped regions considering water compressibility. *J Fluids Eng-Trans ASME* 2015;137(5):051401.
- [103] Xia L, Cheng Y, You J, et al. CFD analysis of the runaway stability of a model pump-turbine. *IOP Conf Ser: Earth Environ Sci* 49. 2016. p. 42004.
- [104] Liu SH, Zhou DQ, Liu DM, et al. Runaway transient simulation of a model Kaplan turbine. *IOP Conf Ser: Earth Environ Sci* 2010;12(1):12073.
- [105] Liu JT, Liu SH, Sun YK, et al. Numerical study of vortex rope during load rejection of a prototype pump-turbine. *IOP Conf Ser: Earth Environ Sci* 2012;15(3):32044.
- [106] Fu XL, et al. Li DY, Wang HJ. Investigation on the fluctuation of hydraulic exciting force on a pump-turbine runner during the load rejection process. *IOP Conf Ser: Earth Environ Sci* 2018;163(1):012101.
- [107] Fan H, Yang H, Li F, et al. Hydraulic torque on the guide vane within the slight opening of pump turbine in turbine operating mode. *IOP Conf Ser: Earth Environ Sci* 2014;22(3):32050.
- [108] Xiao Y, Xiao R. Transient simulation of a pump-turbine with misaligned guide vanes during turbine model start-up. *Acta Mech Sin* 2014;30(5):646–55.
- [109] Stens C, Riedelbauch S. Investigation of a fast transition From pump mode to generating mode in a model scale reversible pump turbine. *IOP Conf Ser: Earth Environ Sci* 2016;49(11):112001.
- [110] Liu JT, Liu SH, Sun YK, et al. Three dimensional flow simulation of load rejection of a prototype pump-turbine. *Eng Comput* 2013;29(4):417–26.
- [111] Côté P, Dumas G, Moisan É, et al. Numerical investigation of the flow behavior into a Francis runner during load rejection. *IOP Conf Ser: Earth Environ Sci* 2014;22(3):32023.
- [112] Yao Z, Bi HL, Huang QS, et al. Analysis on influence of guide vanes closure laws of pump-turbine on load rejection transient process. *IOP Conf Ser: Mater Sci Eng* 2013;52(7):66–71.
- [113] Liu Y, Luo L, Li Q. Study on influence of asynchronous guide vane On the "S" characteristic of pump-turbine. *J Gansu Sci* 2015;27(6):59–63. [in Chinese].
- [114] Li Q, Jiang L, Li R, et al. Numerical analysis of transient process of guide vane opening of pump-turbine. *J Lanzhou Univ Technol* 2015;41(6):60–4. [in Chinese].
- [115] Zeng W, Yang J, Hu J, et al. Guide-vane closing schemes for pump turbines based on transient characteristics in S-shaped region. *J Fluids Eng-Trans ASME* 2016;138(5):051302.
- [116] Hua Y. Analysis of unsteady flow in hydraulic turbine with dynamic mesh technology. Xi'an University of Technology; 2009. [in Chinese].